clean technologies

MDPI

Article

Assertions on an "In Situ" Hydrogen-Powered Ride-On Industrial Floor-Cleaning Scrubber

Leandro Henrique Camargo [1], Renato Rodrigues Silva [1], Yuri Alexandre Meyer [1] and Wislei Riuper Osório [1,2,*]

[1] School of Technology, Campus I, University of Campinas, UNICAMP, Limeira 13484-332, SP, Brazil; renato.silva.research@gmail.com (R.R.S.); yameyer@unicamp.br (Y.A.M.)
[2] Research Group in Manufacturing Advanced Materials (CPMMA), School of Applied Sciences, FCA, Campus II, University of Campinas, UNICAMP, Limeira 13484-350, SP, Brazil
* Correspondence: wislei1@unicamp.br

Abstract

This study proposes a hydrogen-powered industrial ride-on scrubber (IRoS) investigated by using in situ and on-board H_2 production. Technological and financial calculations involving conventional liquefied petroleum gas (LPG), an electric battery, and a hydrogen-powered system in IRoS are discussed. Energy consumption, operational costs, financial aspects and environmental impacts are also discussed. Investment payback analyses to replace an LPG machine are discussed. For 10 years, the highest operational costs and downtime costs are of the LPG-powered scrubber (USD ~187k). The two other systems are substantially lower, i.e., ~4% and 7%. CO_2 emissions of the three examined scrubbers ranged between 162 and 194, 10 and 13, and 5 and 9 tCO_2, respectively. Gravimetric energy density (GED) reveals that the LPG-powered system is ~2× and 10× higher than the battery- and H_2-powered systems, respectively. Adequate modulation and control of the produced H_2 volume in Al hydrolysis are keys to success in the H_2-powered scrubber project. For this purpose, three aspects are important: i. adequate selection of Al-based alloy or mixture powders, ii. the nature and concentration of alkali solution and iii. the quantity of solid (Al-based alloy or mixture powders) per volume of alkali (liquid), designated as S/L ratio.

Keywords: hydrogen-powered fuel cell; industrial scrubber; gravimetric energy density; Al hydrolysis; economic analysis; life-cycle emission

Check for updates

Academic Editor: Damien Guilbert

Received: 11 June 2026
Revised: 9 July 2026
Accepted: 20 July 2026
Published: 5 August 2026

Copyright: © 2026 by the authors. Licensee MDPI, Basel, Switzerland. This article is an open access article distributed under the terms and conditions of the Creative Commons Attribution (CC BY) license.

1. Introduction

1.1. Hydrogen Technology and Fuel Cell

It is unquestionable that the hydrogen-based technology is one of the main renewable energy sources. In global energy transitions, the innovative solutions involving reconciling operational efficiency, environmental sustainability, and economic viability are important aspects. In this subsection and the next two sections (Sections 1.2 and 1.3), the aim is to promote the understanding of H_2-based technologies involving hybrid systems and on-board and hybrid systems, respectively. Hydrogen-based technologies are reported as the central energy systems for decarbonization advances [1]. Hydrogen utilization is suitable for distinctive applications, considering both the stationary and the on-board systems [1]. It represents a low-carbon and viable energy storage, power generation, and transportation [2]. Hydrogen and fuel cells impose a relative cost and performance trajectory similar to those

of solar and battery systems [3]. Hydrogen energy is an important key to replacing fossil fuels, and net-zero gas emissions are intimately associated. Importantly, those remaining and new future conventional combustion engines require low emissions of particulates [4]. In this aspect, hydrogen fuel cell and battery systems seem to be promising alternatives with respect to sustainable and cleaner energy [4].

Although the term fuel cell indicates the concept of PEMFC (proton exchange membrane fuel cell), it is also designated as a hydrogen fuel cell. It plays a pivotal role in the new cleaner energy scenario [5]. Basically, a fuel cell involves physicochemical processes of oxygen diffusion and charge transfer phenomena. Its physical structure is an electrolyte layer in contact with two porous electrodes containing catalyst contents [5,6]. There exists a great number of fuel cell types depending on the fuel, the catalyst material and the electrolyte used. For instance, a direct ethanol fuel cell (DEFC) produces a liquid ethanol–water solution with Pt/Pt-Ru supported on carbon. The electrolyte is Nafion® (a perfluorosulfonic acid solid electrolyte membrane)/alkaline media [6]. A PEMFC produces hydrogen with Pt supported on carbon, and the electrolyte is solid Nafion® [6].

Unlike batteries that store their reactants inside the cell, a fuel cell converts chemical energy into electrical energy. Their reactants are continuously fed to the fuel cell from external stores [6]. Additionally, a battery consumes its electrode irreversibly in a primary cell, and this is reversible in a secondary cell. Also, it does not participate in the reaction [6]. A PEMFC variation is designated as PEMWE (proton exchange membrane water electrolyzer) with a similar PEMFC structure. However, it operates in an opposite process to the PEMFC. It permits protons to migrate from the anode to the cathode (similar to PEMFC) when electricity is applied. This is considered a system with an external or outer circuit. In other words, a PEMFC consumes H_2 and O_2 to generate electricity and water. On the other hand, the PEMWE consumes electrical energy to promote water electrolysis, and both H_2 and O_2 are generated [7,8]. Independent of the kind of fuel cell, the degradation of the core components is the main drawback, which affects both the durability and cycle lifetime. The main components suffering degradation are the membrane, the catalyst layer construction, and the gas diffusion layer [5]. Their degradation occurs mainly due to the thermal cycle being higher than the working temperature. In addition, mechanical and chemical reactions, high voltage, and high gas pressure conditions are also responsible for accelerating degradation [5,9,10].

1.2. Hybrid Hydrogen-Powered Systems

Considering environmentally friendly aspects, the terms zero-carbon, carbon neutrality, decarbonization and net-zero gas emissions are highly requested. In this sense, the concept of hydrogen-fueled systems is a key pathway to this important requirement. Based on this, there are several studies involving methodologies and technologies integrating hydrogen, electric power and battery systems [2,4,10–14]. Hwang et al. [4] have reported that the PEMFC associated with the battery system is an alternative for certain mobility designs. The recognized on-road vehicle systems (e.g., Hyundai NEXO, Toyota Mirai, and Honda CR-V) utilize the PEMFC stack as the main power source for driving and a battery unit as an auxiliary system. On the other hand, when a robust system requires variation in electric energy, e.g., off-road heavy equipment [4], a hybrid PEMFC–battery power system is "quasi-mandatory" [4]. It is demanded not only in mobility systems but also in stationary industrial activities. In systems requiring power with strict frequency (no fluctuations), voltage, and power quality criteria, a hybrid system combining energy storage devices and renewable energy, mainly hydrogen-based, is more promising. It is recognized that the possible intermittency of energy is provided by those commonly renewable energy systems (e.g., solar and wind). This intermittency is frequently attributed to the season,

climate variation and peak charge demand [14,15]. This induces a hybrid system with a more adequate supply of energy and no substantial fluctuations. Zhang et al. [15] have reported a hybrid system constituted by a photovoltaic module, an electrolyzer module and a fuel cell module. A complete conversion process of solar energy is reported [15]. It initiates with absorbed energy by the photovoltaic cell being applied to the fuel cell. Bhutto and collaborators [16] have utilized a model based on the hierarchical control structure to integrate distinctive renewable energy sources. Solar, wind turbine, diesel generator and hydrogen PEMFC constitute this. It is uncontestable that the automobile industry has provided an important pillar for the development of the modern world economy [14]. Also, it is recognized that continuous developments of hydrogen technologies associated with fuel cell electric vehicles have received great attention. Shusheng et al. [14] have demonstrated that the design of the on-board hydrogen-producing fuel cell in electric vehicles is successfully practiced. The system has a burner and reformer, a methanol storage tank and a purifier [14]. The construction of the fuel cell system is mainly constituted by a fuel cell stack, a fuel supply and circulation system, an oxidant (O_2) supply system, a hydrothermal management system and a control system. This guarantees the power output requested in certain applications [14]. A lithium battery pack is also integrated to effectively promote the peak power. However, considering the on-board systems or the intention of portable applications, a chemical hybrid-based fuel cell system seems to be more suitable [17,18]. It promotes a high energy density since energy is generated by an electrochemical reaction [17,18]. In addition, it has an intrinsic eco-friendly aspect, does not produce noise and also does not promote vibration-free operation [17]. Yartys et al. [17] state that the metal hydrides (e.g., MgH_2, $NaBH_4$, $LiBH_4$, etc.) and light metals (Al, Mg or their alloys) deserve special attention. This is because, for the fuel cell supply, the hydrogen is generated directly at the place of its use. They have demonstrated that a fuel cell stack and a hydrolysis-type hydrogen generator using sodium borohydride ($NaBH_4$) have assured efficient operation. It is remarkable that an electronic control unit regulates the hydrolysis reaction rate and hydrogen is modulated to the fuel cell. Also, in the electronic system, supercapacitors are used [17].

1.3. Closed Looping, On-Board or In Situ Hydrogen Production

Based on the hydrogen demanded or required, for systems using compressed hydrogen or that generated from traditional (non-zero-emission) methods (e.g., steam reforming of hydrocarbon carbon), the decarbonization or net-zero gas emissions is substantially far from realization. These systems provide a range of energy higher than 50 kW, as utilized in certain vehicle applications [19]. On the other hand, when systems have limitations in storage space or require a high level of mobility, it seems that a hybrid or closed-loop one is not enough depending on the renewable source adopted. Additionally, under certain conditions, these stockpiles represent a substantial fire hazard depending on the stored and pressurized hydrogen volumes [20]. Thus, for certain applications (portable devices requiring lower than 100 W) [19], a system involving chemical hydrides [1,19–22] promotes adequate and sustainable hydrogen storage. It is noted that there are hybrid fuel cell-based energy systems utilizing metal hydride as hydrogen storage [22]. A hybrid powertrain system involves a PEM fuel cell, a battery pack and an ultra-capacitor pack as power sources. This system runs a hydrogen-powered electric wheelchair [22] ranging between 125 and 1000 W. An electronic control unit to modulate and to control the energy load is used. The metal hydride is utilized as an energy storage device. When a sudden peak demands the system, the electronic control unit activates the ultra-capacitor pack, and the system is adequately supplied. The fuel cell is responsible for recharging the system.

Considering a Li-ion battery, it has specific energy estimated between 125 and 210 Wh/kg. The system utilizing the metal hydride reaches about 400 Wh/kg [22]. Yartys and collaborators [23,24] have also reported metal hydrides for storage and refueling in an H_2-powered fuel cell for utility vehicle applications. It is recognized that the main advantage of metal hydrides under the commonly used hydrogen pressuring/storage systems is their lower storage pressure [23,24]. In a general way, it is recognized that often a fuel cell system does not rapidly respond to power variations. At least, this suggests integration with other energy sources, mainly battery packs, associated with an electronic unit to modulate the dynamic power demand (variations).

Metzger and Li [25] have compared three distinct sources of power for electric forklifts. A Li-ion (particularly $LiFePO_4$, FPO) battery, a PEMFC and a direct methanol fuel cell (DMFC) are compared. Distinct technical and economic aspects are very detailed and discussed. Summarizing, to predict the best choice among the FPO, PEMFC and DMFC, two important aspects are considered: firstly, the fleet size, followed by the infrastructure installed. Considering 10 years as the lifetime cycle, the lowest value is that of the FPO (battery system). Both the PEMFC and DMFC have similar results, but these two systems demand a battery-integrated system. From this point of view, the regenerative fuel cell concept is revisited. Basically, it works with a reverse cycle, using the excess electric power to split water into H_2 and O_2. Sequentially, oxygen is stored and, when demanded by the power required in the system, it is fed back to the fuel cell, generating the power demanded [21]. This implies that a compressor (type twin-head, controlling stoichiometric flow of H_2 and O_2) integrated into the fuel cell is intrinsically required. In addition, the water inside the system is also stored (no external contact) and "electrolyzed" to produce H_2 and O_2.

Miao et al. [13] have utilized a closed, reversible or regenerative system with the metal hydride tanks modulating the hydrogen-powered bicycles. Basically, the hydrogen-to-electricity conversion is successfully attained in road conditions in urban areas. Considering a PEMFC power output of 215 W, the system maintains a stable hydrogen flow rate for over 30 min [13]. Since the 1970s, the concept of a unitized regenerative fuel cell (URFC) consisting of a single cell operating with both the electrolyzer and the fuel cell has been investigated [26,27]. However, due to its poor efficiency and expensive materials involved, its progress has been hindered. Currently, with a relative drop in cost in battery and catalyst materials, attention is focused on the promise of hydrogen-powered systems.

1.4. Contribution and Comparative Hydrogen-Powered Industrial Manned Scrubbers

In this present investigation, the aim is focused on the economic and technical analyses to help in a decision to adopt a hydrogen-powered industrial manned scrubber. It is importantly noted that the proposed system involves an "in situ" and "on-board" hydrogen fuel cell scrubber system. This is considerably different from the more commonly used compressed H_2 fuel cell scrubber system. This is a system recognized and reasonably applied, as utilizing a scrubber embedded with a Power GenDrive® fuel cell model. For instance, a forklift utilizes a hydrogen-powered system [17], and other hybrid systems obligatorily demand compressed hydrogen (>350 or 500 bar) [23,24]. These systems are require pit-stop point to refueling, which includes certain costs and hazard levels.

Despite this matter, the literature is scarce on the technical and economic aspects of an industrial ride-on scrubber (IRoS). Literature reports studies of forklifts, bicycles and wheelchairs. However, the IRoS is absent or scarce, mainly considering H_2-powered in situ and on-board systems. Additionally, alternative routes to hydrogen production can potentially be used. This is intended to modulate the hydrogen rate demanded when load variations are required. For this purpose, a quantitative and comparative analysis

is provided. A conventional liquefied petroleum gas (LPG), an electric battery ($LiFePO_4$, FPO), and a hydrogen-powered ride-on scrubber are evaluated. The corresponding results of the energy consumption, the operational costs per hour, the environmental impacts, and the investment paybacks during 10 years are estimated.

2. Materials and Methods

2.1. Equipment and Technical Specifications

First of all, it is noted that comparisons of certain technical and economic aspects of the three distinctive industrial ride-on scrubbers (IRoS) are adopted. The LPG, battery $LiFePO_4$ (FPO), and hydrogen-powered scrubbers are compared. Although certain limitations are present in these comparisons, it is important to clarify that after energy is converted, its corresponding by-products are relatively different. For instance, the hydrogen-powered system has a by-product constituted mainly by a complex aluminate hydroxide, while battery and LPG systems are free of this by-product. Although this seems to include a maintenance stage (aluminate disposal), which is observed in the LPG and battery systems, the by-product can potentially be reutilized in other industrial applications. In order to standardize the comparisons, all IRoS machine scrubbers are mid-size or medium-size. This corroborates with the comparison of autonomy and operational timing.

The gravimetric energy densities and overall weights of each one of the studied systems are calculated and compared. Additionally, it is worth noting that the comparisons among the LPG, battery, and H_2-powered scrubbers have limitations. This concerns the asymmetry among these systems. For example, the H_2 system generates aluminate (by-product), and its disposal into a container seems to be a reasonable constructional solution. This aluminate can be used in cosmetic and other industrial applications, and its environmental impact seems to be minimized. Concern for the life-cycle of the $LiFePO_4$ battery and its negative impacts on environmental aspects is recognized. However, due to their recycling involving complex stages, this impact is difficult to measure and compare with other ones.

Diesel- or gasoline-powered ride-on scrubbers are commonly used in external areas naturally aerated and ventilated. In addition, these fossil-powered scrubbers intrinsically involve high pollutant emissions. It is estimated that a mid-size ride-on scrubber covers a warehouse, distribution center, or shopping space between 2000 and 10,000 m^2 adequately. This is ergonomically and financially unsuitable for those known walk-back scrubbers. Based on both the qualitative and quantitative analyses, it is intended to help with a decision based on the energetic consumption, operational cost (in monetary units per hour), estimated payback during 10 years, and complexity of the on-boarding system. Obviously, the ESG (environmental-social-governance) aspect is also intrinsically involved. It is important to note that an LPG is adopted instead of a diesel-powered system due to its low environmental impacts with reduced carbon emissions.

Table 1 shows the technical characteristics of the three scrubbers compared. These adopted models are based on Brazilian's market. Another limitation in this comparison concerns the fact that these selected scrubbers have a medium size. For each scrubber, the floor cleaning capacity, covering area, average working autonomy and the gravimetric energy density (energy/overall weight) can be reasonably different. The motor power is difficult to compare due to the different nature, structural characteristics, and possible variation among the different trademarks/fabricants. For instance, the LPG-fueled motor is 55 HP, while the electric (battery) motor has about 16 HP (~3.5 lower). This is a comparison between two different scrubbers, which seems to lead to mistakes in its interpretation. Firstly, the torque needed to carry out a certain task seems to be more important than the working autonomy. In addition, depending on the utilized battery pack, the autonomy

attained can be lower than the initially planned. Although these limitations are mentioned, it is interesting to note that certain and important guidelines are provided, as will be discussed further.

The values applied to energetic consumptions and costs of each one of the energies of the scrubbers are based on supplier/fabricant information and the Brazilian market. Due to this, the converted monetary unit is multiplied by 5, and US Dollar (USD) values are depicted. The specific energy demand (SED) corresponds to the energy necessary or spent to carry out a specific cleaning task. Fuel costs are based on Brazilians' market and average values are shown in Table 1.

Table 1. Technical and specific characteristics involving financial aspects such as operational costs, downtime costs and CO_2 emission data of the three examined types of industrial ride-on cleaning scrubbers.

Technical Characteristics		LPG (Conventional)	Battery (Electric)	Hydrogen (PEM)
Technology involved		Engine combustion motor	Battery 36 V	PEM fuel cell + battery auxiliary
Fabricant/Model		Tennant (Minneapolis, MN, USA), T20, motor 55 HP, tank 33lb (15 kg).	Factory Cat GTX (Racine, WI, USA), 36 V, 245–325 Ah	Nilfisk (Minnesota, MN, USA), Advance CS7000 PEM Plug Power GenDrive®, Series 3000
Specific energetic demand (SED)		2.5~3.0 kg LPG/h	1.18~1.56 kW/h	0.059~0.094 kg(H_2)/h
Autonomy (h)		5	7.5	Full
Net energy (NE) (1)		~41 kWh	~7.8 kWh	~20 kWh (2)
System weight (kg) (3)		~31	~120	~200
Gross vehicle weight (GVW) or overall weight (kg) (4)		~2200	~800	~2800
Gravimetric energy density (GED; GED_t) (5)		GED = 1.3 kWh/kg	GED = 0.6 kWh/kg	GED = 0.1 kWh/kg
		GED_t = 18.6 Wh/kg	GED_t = 9.7 Wh/kg	GED_t = 7.1 Wh/kg
Energy source cost (USD)		2~3/kg (6)	0.15~0.20	2.80~4.00
Relative CapEx		1	1.67	3.17
Relative annual OpEx		1	0.56	0.74
SED cost range (USD/period)	1 h	5~9	0.17~0.31	0.17~0.38
	40 h	200~360	6.8~12.4	6.8~15.2
	10 years	104.0k~187.2k	3.5k~6.4k	3.5k~7.9k
Relative SED cost for 10 years (USD)		1	0.033~0.034	0.033~0.042
Downtime for refueling (min.)		5	20 (rapid); 480 (full)	3
Estimated DT for 40 h (in hours)		0.67 h	1.78 h; 42.7 h	0.050 h
Estimated DTC (10 years), USD		347~540.80	924~2.4k; 57.7k	26~128.18
LDT (labor downtime), USD		1.56	2.6	4.93
SED + DTC (10 years), USD		104.3k~187.7k	4.4k~8.8k 64.1k (480 min recharging)	3.5k~8.0k
CF (correction factor for CO_2)		3.1167	0.4038	4 (recyc.); 36 (renew.); 132 (prim.)

Table 1. *Cont.*

Technical Characteristics		LPG (Conventional)	Battery (Electric)	Hydrogen (PEM)
Emission CO_2	40 h	312~374 kg	19~26 kg	10.5~16.8 kg
	10 years (ton.)	160~194 ton	10~13 ton	5~9 ton
	Relative	1	0.06~0.07	0.034~0.045
CO_2/GED_t ratio		20.1 $kgCO_2/Wh/kg$	2.7 $kgCO_2/Wh/kg$	2.4 $kgCO_2/Wh/kg$

(1) Net energy (NE) values are obtained from each supplier according to the models considered, except for the H_2 system. (2) Net energy of the H_2 system is calculated based on 1.1 kg H_2 under 350 bar (pressured cylinder), resulting in a gross storage energy of ~36 kWh. Using a PEMFC (60%), the resulting NE is ~20 kWh. (3) System weight is that of the corresponding LPG cylinder (~15 kg) + mass of LPG (~16 kg); and 6 batteries (~180 kg) and their secondary devices (cables + converter/inverter); and H_2 cylinder and devices (~150 kg) for LPG-, battery- and H_2-powered systems, respectively. (4) Gross vehicle weight means the overall weight or total mass considering all components constituting the scrubber system, i.e., water dispensers, brushers, dirty dispenser, tires, metallic structure, etc. This corresponds with "real" weight filled and full capacity. (5) This corresponds with NE per system and overall weights, respectively. (6) Global Petrol Prices (www.globalpetrolprices.com/pg_prices/; accessed on 12 April 2026) commonly provides prices per liter, and it should be considered that 1 kg has ~1.96 L. Also, it should be considered that chemical composition and its mixture. For this reason the value in the table is shown in a range based on the variation in composition and distinctive countries.

LPG has a cost between USD 5.00 and 9.00/h, considering its consumption based on demand calculated [28]. On the other hand, the electric energy for its total recharging has a cost between USD 0.15 and 0.20. This takes into account the tariff rates applied to customers with the specific industrial demand. The hydrogen range price is between USD 2.8 and 4.00 per hour depending on the supplier selected. This is based on the typical efficiency of the fuel cell system. Additionally, the hydrogen consumption of 0.059 and 0.094 kg per hour corresponds with the scrubber per the shift carrying out certain cleaning tasks.

Importantly these values can be substantially modified or different when distinctive countries and economies are considered. This promotes a reasonable understanding of the comparisons made and the trend achieved. Considering the estimated values of the refueling for all three examined sources, these are based on the minimum cycle times to recharging or refueling.

2.2. Total Cost of Ownership Determination

It is remembered that the aim of this investigation is not focused on an exhaustive and detailed economic analysis with deeper accountability numbers. It is intended to clarify some parameters and to promote comparisons to future buyers, suppliers and users. This is associated with future technology with lower pollutant emissions. Immeasurable profits are directly associated with these "green fuel systems", and a simple formula to indicate profits or revenues seems to promote equivocal interpretations and decisions.

The Total Cost of Ownership (TCO) calculation is commonly used to determine all costs involved. In addition, comparisons among the different powered fuels [29], e.g., diesel, LPG, battery and hybrid models [29,30] can also be provided. Commonly, it involves a great number of costs, e.g., the purchase cost, financing and depreciation (direct and fix cost). Added to these, the consumption, insurance, maintenance and repairs are other additional costs. Simplifying, the TCO considers initial purchase and the secondary costs (financing and fees) as fixed costs. These are added to the fuel costs and the insurance and maintenance costs (variable costs) over 10 years. Thus, the CapEx and OpEx concepts are brought to the forefront, meaning the costs associated with the scrubber acquisition (purchasing cost) and operational costs. However, it is again noted that these costs are not detailed and individually described, but simplified and designated as the CapEx and OpEx. Annual OpEx values are obtained by using those monthly values multiplied by 12. The CapEx and OpEx costs are added to the annual depreciation of each one of the scrubbers considered. These represent the annual rates of about 8.3, 10 and 5%, respectively.

2.3. Cash Flow (CF) and Payback Period (PP) Determinations

In a general way, as financial indicators, the cash flow and the payback period parameter are adopted. It is recognized [31] that there are other financial indicators, e.g., net present value, profitability index and internal rate of return [31]. However, only the cash flow (CF) and the payback period (PP) indicators are adopted. From the financial point of view, and considering the period required for the net cash flow to attain or offset the initial total investment, there are two distinctive parameters. One is designated as the Static Payback Period (SPP), and another as the Dynamic Payback Period (DPP). These define the period required for the net cash flow to offset the initial TCO without considering the time value. Another takes into account the time value of money over the years and interest, respectively. These are determined by using Equations (1) and (2), respectively.

$$\sum_{j=1}^{SPP} CF_j - C_{cap} = 0 \tag{1}$$

$$\sum_{j=1}^{DPP} CF_j(1+i_{real})^{-j} - C_{cap} = 0 \tag{2}$$

where CF_j is the cash flow at year j including CapEx and OpEx annual values, C_{cap} means the initial total capital investment cost and i_{real} is the annual real discount rate involving the nominal discount and the inflation rate, also called the "hurdle rate" or the minimum attractive rate of return [31].

This is considered only in the DPP calculation; in other words, it considers "devaluation" of money over time, being more "realistic" than the SPP value. The i_{real} is adopted in a range between 15 and 25% since the hydrogen technology is relatively new for scrubber machines. This range is based on the previous comments concerning equipment application, market drivers and operational dynamics into Brazilian's market [32]. This varies depending on the countries and their adopted economies. For instance, in the USA market, between 5 and 8% is adopted [33]. The mentioned numbers are associated with a medium-to-high risk premium and the policy rate or benchmark interest rates. For instance, this is different when Fed funds in the USA, Selic in Brazil, Base rate in England, etc., are considered.

2.4. Downtime Cost (DTC) and CO_2 Emission (E_{CO2}) Determinations

It is remarkable that the DTC ranges are estimated. These are based on the period to refueling (or recharging) of the examined LPG-, battery- and H_2-powered scrubbers. The estimated downtimes are based on the corresponding refueling/recharge period times, i.e., 5, 20 and 3 min, respectively. It is remembered that the refueling or recharging of the battery system can have different ranges, varying between 20 min. up to 480 min. (8 h). In the last case, a catastrophic final cost can be achieved.

The DTC (Downtime cost) values are determined by using Equation (3). The working shift of 40 h divided by the corresponding downtime (minutes converted to hours, i.e., dividing by 60) of each different scrubber (i.e., LGP, battery and H_2) is considered. This is multiplied by the downtime cost and extrapolated to 1 h, 40 h or 10 years (20,800 h). This period is coincident with a possible cycle lifetime of the examined machines.

$$\text{DTC} = \frac{WS_{(40h)}}{A} \cdot \frac{DT_{min.}^{Ref.}}{60} \cdot \frac{20,800}{40} \cdot LDT \tag{3}$$

where $WS_{(40h)}$ is the 40 h of work shift, the term A is autonomy (in hours) to carry out the determined cleaning task, the $DT_{min.}^{Ref.}$ is the downtime for the refueling (in minutes) and

20,800/40 (i.e., 40 h × 52 weeks = 2080 h/year) is used to extrapolate 10 years considering a work shift of 40 h; and the LDT is the labor downtime cost (in USD).

It is recognized that the calculation of the LDT cost is complex, and under certain conditions these values are extrapolated or underestimated. This is due to the fact that a real or very close to real cost involves the lost quantity of pieces (unproduced component units) in stopping periods (downtime). For simplification, the following method is adopted to achieve the DTC values. The CapEx is divided by the cycle lifetime of each piece of equipment, added to the man-machine hour, specifically the Idle Man-hour (IMH) or the labor downtime or the waiting time to carry out the refueling/recharge. It is noticed that no "maintenance" costs are taken into account.

The CO_2 emission (E_{CO2}) calculations are made by using the SED_x, meaning the specific energetic demand to carry out a certain cleaning operation per hour multiplied by a correction factor (CF_x), as described in Equation (4).

$$E_{CO2} = SED_x \cdot CF \tag{4}$$

where the subscript "x" in both the SED (energy unit per hour) and the *CF* corresponds to the three different powered sources on-boarding the scrubbers, i.e., SED_{LPG}, $SED_{Batt.}$ and SED_{H2}.

When considering LPG as an energy source for the scrubbers, the term SED_{LPG} is multiplied by a carbon fraction (cf = 0.85). This is due to LPG as a fuel source having its chemical composition constituted by the propane and butane contents. The carbon content is different in each gas. Thus, a stoichiometric proportion to convert carbon to CO_2, i.e., molar ratio (44/12, in g/mol) between CO_2 and carbon, is used [31,34]. In the literature, other methods to determine the E_{CO2} are also used [31]. These utilize the emission coefficient [31,34,35], the low calorific value and the fuel consumption of thermal power generation. For simplification, and due to the variability of the LPG composition, the results attained by using Equation (4) substantially corroborate the magnitude of CO_2. When the battery system is considered as the energetic source, and to determine the amount of E_{CO2} emission, Equation (4) is replaced with $SED_{Batt,}$ and the *CF* is described by Equation (5).

$$CF_{Batt.} = (1 - Je) \cdot ef \tag{5}$$

where SED_{Batt} is the specific energetic demand per hour (in kW/h), the parameter "*Je*" is the Joule effect (in %) due to the heat generated in conversion depending of the (re)charge technology used (commonly between 15 and 20%); and the *ef* depends directly of the utilized electrical matrix (the generator origin) and the country where the recharge is carried out.

Since an industrial environment is considered, winter and summer have no substantial effects on the final result. This is because no variation in the tariff is applied, which commonly occurs in domestic tariffs. Globally, the parameter *ef* is 0.475 kg CO_2 per kWh [36,37]. Considering the average Brazilian's emission factor, this value is up to 10 times lower (~38.5 kg CO_2 per MWh) [38], according to the National Interconnected System (SIN) in Brazil [38]. This is because different energy matrices are practiced in the USA, Europe, and Brazil.

When hydrogen is considered as the source, its corresponding CO_2 emission at the local or site of reaction is theoretically "net-zero" or "close-zero" emission. However, since Al hydrolysis is taken into account, it depends entirely on the carbon footprint related to the source of the aluminum used. Aluminum can be primary, secondary or from recycled alloys. From the theoretical calculation, 1 kg of aluminum produces about 112 g of H_2 with water [39]. Considering CO_2 emission, 1 kg of Al produces a quantity of CO_2 strongly

dependent on the production source, i.e., coal, hydroelectric, etc. [39]. This means that primary Al commonly (global number) produces ~15 kg CO_2. When a renewable source is considered, this quantity decreases to ~4 kg CO_2, and a quantity of about 20 kg CO_2 when the coal as main source is used [38,39]. A substantial decrease in the CO_2 emission is achieved when the recycled Al alloys are utilized (~0.5 kg CO_2/kg Al) [40,41]. Based on this, the amount of CO_2 emission by using hydrogen in a fuel cell, considering Al hydrolysis, the term *CF* described in Equation #4 is replaced with (14.8/0.112 in kg CO_2 to H_2), which converts 1 kg Al to CO_2 (as Al primary) and to CO_2. Evidently, if the Al source is from a renewable source, this value must be replaced with "4/0.112", as aforementioned. Simplifying the analysis, all three *CF* values and E_{CO2} results corresponding to the LPG, battery and hydrogen are shown in Table 1.

2.5. Al + Sn and Al + Bi Powders Mixtures: H_2 Production in NaOH

By using the Al hydrolysis concept, the portions (3 and 10 wt.%) of two distinct solutes, i.e., Sn and Bi powders, are mixed with Al powder portions. This in order to measure the resulting hydrogen volume yields. These powders are selected for two reasons: i. to promote comparisons with the previous studies; and ii. to demonstrate the distinct nature and electrochemical characteristics of the two powders affecting the H_2 volumes generated. This implies that controlling or modulating "in situ" and "on-board" H_2 production constitutes a potential mechanism to supply adequate volumes to a PEMFC system. This will be discussed further. For this experimentation, a 0.4 g mass of the Al + Sn and Al + Bi mixtures is used.

When the percentage of 3 wt.% is selected, 0.388 g Al powder is adequately mixed with 0.012 g Sn and/or Bi. When 10 wt.% is adopted, a mass of 0.360 g Al + 0.040 g (Sn or Bi) is used. Also, two distinct NaOH molarities, 0.25 M (or g/mol) and 0.5 M, are used. This corresponds to 5 g NaOH diluted or dissolved into 250 mL distilled water, and 5 g NaOH in 500 mL of distilled water, respectively. This variation in molarity can also be used as operational variables to modulate and to control the process.

3. Results and Discussion

3.1. Total Cost of Ownership (TCO) Results

As aforementioned, the TCO represents a financial indicator contributing to future decisions of buyers and users. Thus, potentially, different and renewable or "green" energy sources can promote immeasurable profits. In a general way, these "benefits" are not directly obtained or calculated in a simple formula. The TCO indicates all the costs associated with certain equipment, machines and vehicles during their entire lifetime. It facilitates a direct comparison among distinctive models and different fuel-powered vehicles [29]. Some studies have utilized the TCO to compare powertrains of different fuelled trucks (e.g., diesel, battery and hybrid models) [29,30]. Summarizing, the calculation of the TCO involves a great number of parameter costs. It involves the simple purchase cost, financing and depreciation as direct costs. Also, it involves the consumption, insurance, maintenance and repairs [29]. Other costs such as annual registration fees can also be taken into account depending on the purchased equipment, machine or vehicle, as reported by Magnino et al. [29]. They have stated that the TCO summarizes all costs in a unique indicator. As aforementioned, for simplification in the TCO determination, the initial purchase and financing, and fees (fixed costs) are added to the fuel cost and the insurance and maintenance costs (variable costs), considering a period of 10 years. The CapEx and OpEx costs are added to annual depreciation of each of the scrubbers considered, as previously mentioned. It is noted that the initial purchase of each scrubber can be substantially different when different countries are considered. Thus, the relative costs are

taken into account by relativizing each of the CapEx values. Comparatively, the average relative CapEx values corresponding to the LPG, battery and H_2 scrubbers are 1, 1.67 and 3.17, corresponding to USD 24k, 40k and 76k, respectively.

Figure 1a shows the relative TCO analysis considering the three distinctive industrial ride-on scrubbers (IRoS), i.e., LPG-, FPO battery- and hydrogen-powered by utilizing a potential fuel cell, as will be discussed further. Only evaluating this financial indicator, it is confirmed that the initial purchase of an H_2-powered scrubber is relatively more expensive than the other ones. When comparing the battery-powered scrubber with the LPG-powered scrubber, a period of more than 8.8 years is required to "equalize" or to attain the "break-even point" of the investment compared to the LPG system. When no depreciation index of the equipment is considered, an equivocated or flawed analysis can lead to an erroneous decision. It is worth noting that the annual depreciation is considered. This takes into account the relative CapEx of each machine per its corresponding relative lifetimes, as shown in Table 1. Due to the different countries' economies and markets, it is also important to note that the distinct depreciation indexes and CapEx and OpEx costs can be taken into account. This point constitutes a limitation of this study. However, since the relative comparisons are provided. These relative values can be extrapolated to different economies and financial conditions, which will promote indicative perceptions to corroborate the final decision in the capital investment.

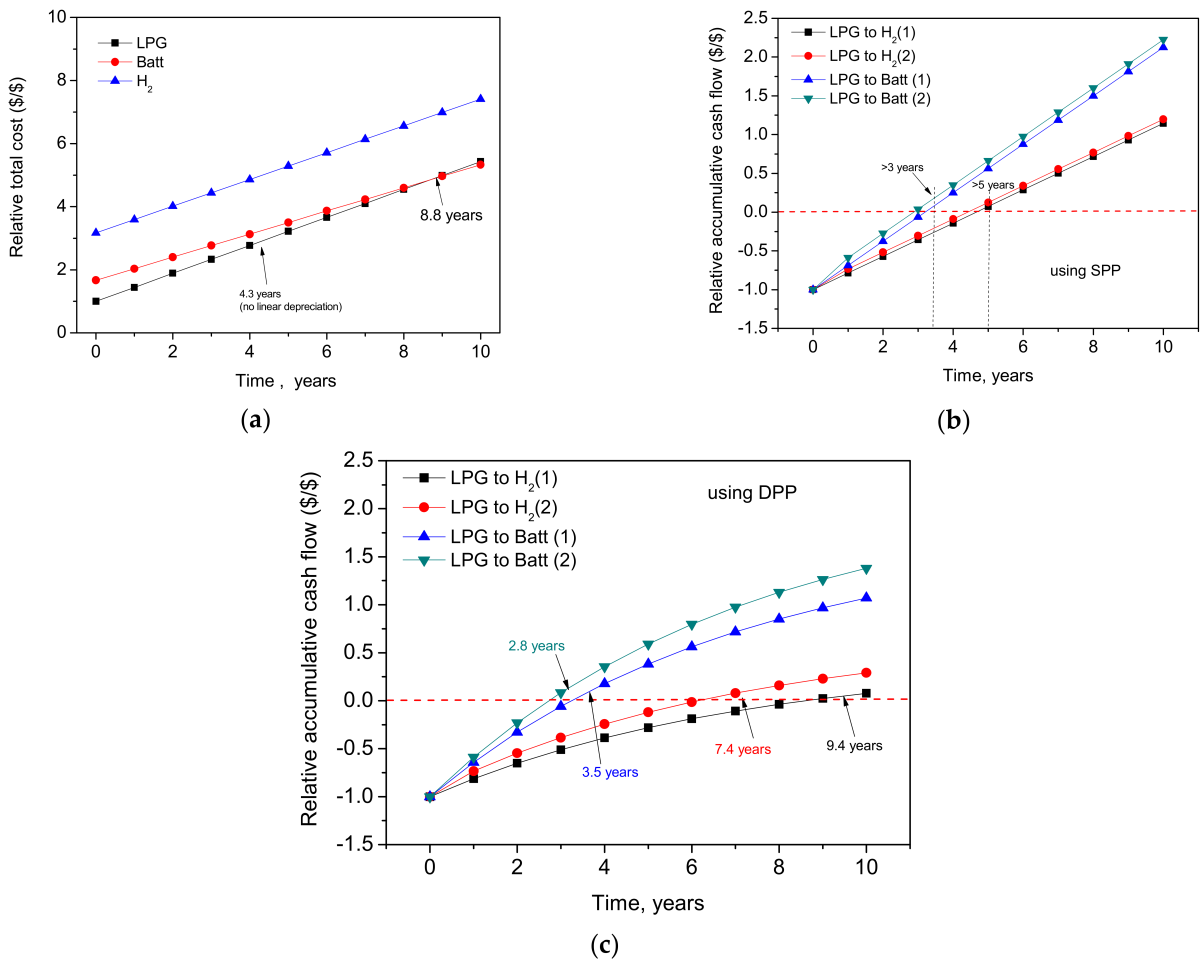

Figure 1. (**a**) The relative TCO (total cost of ownership); and typical results of the relative cumulative cash flows during 10 years considering: (**b**) the static (SPP) and (**c**) the dynamic (DPP) paybacks of the three distinctive industrial ride-on scrubbers (IRoS), i.e., LPG-, battery- and H_2-powered.

With these assertions, it seems that only determining the TCO results, it strongly discourages the desire to adopt the hydrogen technology. It is recognized that cutting-edge products generally involve higher costs and launch prices (new products). However, there are other complementary aspects to be evaluated. Only considering the capital investment or the financial expenditure without an environmental footprint (carbon footprint), the planning for eco-friendly responsibility can be inhibited. In this sense, a more "in-depth analysis" is required; other "hidden" parameters and indicators should be taken into account.

Figure 1b,c reveal the typical results of the relative cumulative cash flows per time during 10 years. Based on these results, the payback values corresponding to the LPG-, battery- and H_2-powered systems are determined. Both the static (SPP) and the dynamic (DPP) payback periods are shown. Two cumulative cash flows per period, represented by "(1)" and "(2)", are shown. Although the relative cash flow vs. time curves are compared, these two curves are obtained when the ranges of both the SED cost and the annual OpEx are considered.

The GLP price ranges between USD 2 and 9 multiplied by 2000 (in hours) to extrapolate to annual cost. This value is added to its corresponding annual OpEx value, totaling between ~USD 16.3k and 20.3k. In the case of the battery, this range is between ~USD 12.5k and 16.5k. By using Equations (1) and (2), the relative cumulative cash flow results of both the SPP and DPP are determined. The red line represents break-even. This graphically represents the minimum period to become positive the initial capital investment. It suggests that more than 3 years and more than 5 years correspond with the payback for "SPP" in order to replace the LPG with a battery; and the LPG with H_2. However, when the DPP is considered, the replacement of the LPG with H_2 has a higher or longer payback. This is also observed when the static payback is analyzed. Conceptually, a DPP takes into account an annual i_{real} tax involving the nominal discount and the inflation rate, also called the "hurdle rate". This leads to a "devaluation" of money more realistic than the SPP calculation. For this study, an i_{real} rate of 15% is adopted [32,33], as aforementioned and justified. This is associated with a medium-to-high risk premium and the policy rate, which is different in distinct countries and global economic conditions, e.g., the global economy chokepoint of the Strait of Hormuz.

3.2. Downtime and CO_2 Emission Costs

As aforementioned, the downtime cost (DTC) is a financial indicator that help to decision of determined project with a friendly financial return. This study promotes other analyses involving the specific energetic demand (SED) of each type of scrubber and its corresponding operational costs. Associated with these costs, the downtime costs (DTC) and those related to CO_2 emission (E_{CO2}) are also involved. Individually, the SED and the DTC represent the cost of energy to carry out a certain task and the time to recharge or refuel the equipment to carry out the task. For this reason, the parameter SED + DTC is further analyzed. In a determined period, the SED + DTC means the total cost to carry out a complete cycle of tasks and its recharging period. Obviously, the OpEx cost should not be neglected since its mean substantial costs when compared with SED and DTCs, as will be discussed further.

Another negative aspect associated with the H_2-powered systems and their financial balance concerns the fact that the majority of H_2-powered projects involve hybrid models (e.g., involving wind or solar energy sources). These are integrated with a battery pack to effectively be connected to H_2 systems to supply the fuel cell energy [22–27]. This leads to a hybrid system containing three parts (renewable, battery and hydrogen). This is relatively complex in terms of the constructional or structural aspects, and leads to relatively

higher costs. These systems have distinctive energy autonomy and consequently different downtimes for refueling or recharging. These refueling times can lead to incommensurable or catastrophic results in total costs. The downtime cost for refueling and its corresponding labor downtime cost (LDT) have been previously commented on. It is recognized that the calculation of these values is complex. In this study, a simplification is adopted. The values corresponding to the CapEx are divided by the cycle life of each scrubber. In addition, the man-machine hour, also called the Idle Man-hour (IMH), associated with the spent time to carry out the refueling/recharge is also taken into account, as previously discussed. This also constitutes another limitation of this study. This is because the IMH values adopted are about 35% [42–44] of the initial capital (CapEx) corresponding to the three different scrubbers. This adopted percentage is based on the Brazilian's market, and it constitutes another limitation in the study [42–44]. For example, the LPG –powered scrubber has its LDT being its CapEx divided by 20,800 h to attain a period of 10 years, added to 35%.

Table 1 depicts the important technical and financial parameters to promote the analyses concatenating the capital investments, monthly costs extrapolated to annual costs and 10 years of total costs. It is also importantly noted that the downtimes for the refueling and the SED costs during 10 years reveal very interesting total costs. These are associated with the CO_2 emission values and seem to provide a different vision for adopting hydrogen technology. For example, when only the initial CapEx and its corresponding paybacks are considered, all indicators suggest that the LPG scrubber is financially viable. Consequently, it is inferred that an H_2-powered scrubber is unable, as shown in Figure 1. On the other hand, when the SED and DTCs are evaluated, the highest SED cost is that of the LPG-powered scrubber. It attains a range between USD 104k and 187k. At this point, the OpEx costs are neglected. These costs will be analyzed further under three distinctive conditions. Considering the SED and DTCs, both the battery- and H_2-powered scrubbers have their costs substantially lower (~4% and 7%, respectively) than the LPG.

When the LPG-powered machine technology is considered, values related to the downtime cost are noticeable, which reach only about USD 540.80 in a period of 10 years. This. When the battery-powered machine is analyzed, the resulting financial number attains a catastrophic level. This depending of the type and charging efficiency of the battery packs utilized. To clarify this assertion, the calculation of the SED cost is more detailed and commented on. The SED cost is calculated by using the SED multiplied by its energy source cost, and it is extrapolated to the working shift of 40 h and 10 years (multiplying by 20,800 h). As aforementioned, it is important to remember that the SED represents the cost of energy to carry out a certain task. The DTC means the time to recharge or refuel equipment to carry out a certain cleaning task. When the SED + DTC are considered, the total cost to carry out a complete cycle of tasks and its corresponding period to recharge are taken into account. For the determination of the downtime costs, Equation (3) is adopted. Basically, three parts constitute the DTCs, and exactly the medial part of the equation has a critical and very important role in computing the final cost. The term $DT_{min.}^{Ref.}$ corresponds to the "stopped time" to carry out a refueling or recharging (in minutes). Considering a 40 h working shift, the autonomy of 7.5 h, and the recharging times of 20 min (rapid), the DT is about 1.78 h. On the other hand, when up to 480 min (slow charging) of the traditional recharging technology is used, a period time of 42.7 h is required. When these values are extrapolated to 10 years, the SED cost is four times higher (~USD 2400.00) than the LPG scrubber. A worst scenario is attained when a recharge of 480 min is utilized. A SED cost of about USD 57,700 is achieved (i.e., higher than 100 times). For this reason the term catastrophic was previously utilized. Interestingly, when an H_2-powered scrubber is analyzed, the lowest SED cost (~USD 128 during 10 years) is attained. It is importantly noted that Al source and NaOH prices are included in the range of the SED costs. The SED

costs are intimately associated with the 1st term of Equation (3) previously shown. In a work shift of 40 h, due to its highest autonomy (full-time 40 h), mathematically its "stopped time" during 40 h is asymptotic to zero, i.e., ~0.05 h during a 40 h working shift. Although a similar refueling time with the LPG-powered system is observed, the LDT is about 1.9× and 3.2× higher than the battery and the LPG, respectively. Remembering that the LDT is a small portion (or negligible fraction) of the DTC, as previously described. When the results of the estimated DTCs during 10 years are compared with their corresponding SED costs also during 10 years, another strategic indicator (in percentage) is revealed. It suggests that the operational cost "supplants (or surpasses)" the downtime costs.

Another interesting parameter involves the SED cost + DTC during 10 years. This reasonably demonstrates that the highest total cost is that of the LPG-powered scrubber system, i.e., it is between ~USD 104.3k and 187.7k. This is followed by the battery-powered system, ranging between USD 4.4k and 8.8k; and the H_2 scrubber system, which ranges between ~USD 3.5k and 8k. When a slow recharge system is utilized, the battery-powered system has a SED + DTC substantially increased, i.e., attains about USD 64k. This value is up to ~18x higher than the H_2-powered system. However, the LPG system is still about 1.6 to 3 times higher than the battery system. The OpEx costs are substantially higher than the SED + DTC, which is further analyzed and discussed.

Considering the environmentally friendly aspects of the three LPG-, battery- and H_2-powered systems, specifically when the CO_2 emissions (E_{CO2}) are determined. It is important to clarify that E_{CO2} is calculated by using Equations (4) and (5), as in the case of the battery system. Also, it is remembered that CO_2 is not a direct pollutant, but it has an important role in the increase in global temperature. All three energy sources directly or indirectly produce CO_2 emissions.

As aforementioned, LPG, as an energy source, has a composition varying between propane and butane, and no 100% is converted directly to CO_2. Thus, a carbon portion of 0.85 and a molar ratio (44/12, in g/mol) are adopted [31,34]. This results in a CF correlated with the LPG, battery and H_2 of 3.12, 0.40 and 4 (considering a recycled material), as shown in Table 1. The CF = 4 corresponds to the H_2 system, and it is associated with the recycled material. This value is modified to 36 or 132 when the renewable energy source and the primary materials are utilized, respectively.

Since the CF = 3.12 for the LPG system is used, the CF = 0.40 correlates with the battery-powered system. Equations (4) and (5) are necessary to determine the E_{CO2} results. Thus, the SED is multiplied by CF = 0.40. The attained value is multiplied by a coefficient of 0.475 kg CO_2 per kWh, which is globally adopted [34,37]. These values are substantially different depending on the country and the energetic matrix utilized; e.g., in South Korea this value is 0.58 kg CO_2/kWh [37]. Although previously discussed, when the H_2-powered system scrubber is considered, three distinct CF values are adopted. Theoretically 1 kg Al generates about 112 g of hydrogen. The amount of CO_2 produced with 1 kg Al is strongly dependent on the origin of the energy source adopted. For instance, utilizing primary aluminum, ~15 kg CO_2 is produced [36–39]. When a renewable source (wind, solar or hydroelectric) is used to produce 1 kg Al, ~4 kg CO_2 is generated. By using coal as the energetic matrix to produce 1 kg Al, the CO_2 emission is about 20 kg CO_2. When 1 kg of recycled aluminum is used, approximately 0.5 kg CO_2 is generated [39–41].

In Table 1, the CO_2 emission values are depicted for 40 h of working shift and over 10 years. Analyzing the relative CO_2 emission among the three powered systems, i.e., the LPG, battery and hydrogen, the battery and the hydrogen systems exhibit substantially lower values than the LPG system. These range between 0.06 and 0.07 and 0.03 to 0.05, respectively, as shown in Table 1. Over 10 years, the LPG-powered scrubber system generates between 162 and 194 ton CO_2 against about 10 and 13 ton of the battery system

and between 5 and 9 tons of CO_2 from the H_2-powered system. A medium-sized automobile (passenger car) with an internal combustion engine of 1.4 to 1.6 L (overall weight ~1.5 up to 1.8 tons) has a resulting CO_2 emission between 11.5 and 15 kg CO_2 [45–48]. When ethanol is utilized, the value ranges between 8.5 and 11 kg CO_2 [45–48].

It is worth noting that emissions are commonly described in kg CO_2/km or g CO_2/gallon. Thus, the stoichiometric conversions are necessary. These values are based on mixed city-highway driving conditions and only emission by exhaust system [45–49]. It is noted that the measurements in the laboratory are substantially different from those obtained during real on-road usage [48]. Also, the automotive engine exhaust generates other pollutant gases such as CH_4 and N_2O [48]. Considering certain limitations and approximations, when the CO_2 emissions by vehicle (gasoline or ethanol) during 10 years are extrapolated, these emissions are higher than a LPG-powered scrubber. Interestingly, these scrubbers (~1500 kg, e.g., Nilfisk (Minnesota, MN, USA), SC8000 LPG or Tennant (Minneapolis, MN, USA) T20 LPG [50]) have a similar overall weight to the passenger vehicles (~1800 kg). Vehicles with 1,500 and 2,000 kg produce between 7 and 15 tCO_2 [48,51]. It is importantly noted that the three examined scrubbers have distinct net energy (NE) values, as shown in Table 1. The NE is the useful energy available or delivered to a machine or motor system after subtracting all thermodynamic and mechanical losses. It is obtained from the heating value (or calorific value) multiplied by the mass of the energy source. In the case of the battery system, it represents the gross nominal capacity (i.e., Ampere-hour multiplied by voltage used) multiplied by the motor efficiency (electric is between 88 and 90%). In the case of the H_2–powered system, a cylinder under ~350 bar contains ~1.1 kg H_2 multiplied by 33.330 Wh (lower heating value), and subtracting PEMFC efficiency (50~60%), the NE is about 20 kWh, as shown in Table 1. With these assertions, as expected, due to the high heating value (or calorific value) of the LPG (12.8 kWh/kg), the highest NE is that of the LPG-powered system. Although the efficiency of the combustion engines (between 28 and 40%) is lower than that of an electric motor (between 88 and 90%); and the LPG has exhibited the highest NE.

On the other hand, all examined industrial scrubbers have different gross vehicle weights (GVW), as also shown in Table 1. This is associated with the on-board constructional structure and technology, e.g., the water dispensers, dirty-water tank/dispenser (recovery tank), brushers, tires, metallic structure, etc. The gravimetric energy density (GED) values of the three examined scrubbers are determined and shown in Table 1. It is worth noting that this parameter means the actual energy that the machine carries per kilogram of "curb" weight. A high GED leads to a lighter machine, demanding lower energy to dislocate than a machine with low GED. For example, a conventional Pb-acid battery-powered system has low GED (i.e., of about 35 Wh/kg). This requires a recharging time higher than 8 h and can take up to 12 h. The estimated values of the GED of the LPG-, battery- and H_2-powered systems are about 1.3, 0.6 and 0.1 kWh/kg, respectively. For instance, the LPG has an LPG mass and a cylinder tank total of about 31 kg, while the battery and H_2 systems are ~120 and 200 kg, respectively. All these GED values are higher than those of the lead-acid battery. When the total weight or gross vehicle weight (GVW) values are considered, the corresponding GED_t (t = total), the same tendency is observed, i.e., the GED_t of the LPG is higher than the battery, followed by the H_2 system. A high GED_t permits the machine to supply the same working shift with lower weight or the lowest recharging or refueling time. As an example, the model Advance CS7000 PEM (H_2-powered system) has the highest GVW (~2800 kg), which is associated with their higher capacity tanks than other ones.

In the last row of Table 2, a relation between the CO_2 emission levels and the GEDt is determined. This represents an "eco-efficiency" parameter that is based on a 40 h working shift. It correlates the pollutant emission mass (in kg CO_2) per unit energy capacity

based on the total machine weight [51]. It is found that the LPG-powered system produces ~20 kg CO_2 per Watt-hour produced per kilogram constituted by the GVW. Both the battery- and H_2-powered systems are about seven and eight times less polluting per energy utilized per kg of their total weight [51].

Table 2. Simplified sensitivity analysis considering the SED, OpEx and DTC for the three examined types of industrial ride-on cleaning scrubbers.

Cost Component	LPG (×1000 USD)	Battery (×1000 USD)	H_2 PEM (×1000 USD)
Capital Expenditure (CapEx, Initial TCO)	24.00	40.00	76.00
SED costs (10 years)			
Optimistic Scenario (−15%)	88.40~159.12	2.98~5.44	2.98~6.72
Baseline/Realistic Scenario	104.00~187.20	3.50~6.40	3.50~7.90
Pessimistic Scenario (+15%)	119.60~215.28	4.03~7.36	4.03~9.09
OpEx costs (10 years)			
Optimistic Scenario (−15%)	367.20~403.75	204.00~224.40	271.32~298.45
Baseline/Realistic Scenario	432.00~475.00	240.00~264.00	319.20~351.12
Pessimistic Scenario (+15%)	496.80~546.25	276.00~303.60	367.08~403.79
DTCs (10 years)			
Optimistic Scenario (−15%)	0.29~0.46	0.79~2.04	0.02~0.11
Baseline/Realistic Scenario	0.35~0.54	0.92~2.40	0.03~0.13
Pessimistic Scenario (+15%)	0.40~0.62	1.06~2.76	0.03~0.15
TOTAL (SED + OpEx + DTC)			
Optimistic Scenario (−15%)	455.89~563.33	207.76~231.88	274.32~305.28
Baseline/Realistic Scenario	536.35~662.74	244.42~272.80	322.73~359.15
Pessimistic Scenario (+15%)	616.80~762.15	281.09~313.72	371.13~413.02

Revisiting the cost analysis in Table 2 a simplified sensitivity analysis considering the SED, OpEx and DTCs is depicted. This analysis is expressed in monetary units (X 1000). The corresponding CapEx values are also shown. Three distinct scenarios are forecast (i.e., the actual or baseline, optimistic and pessimistic). Based on the actual scenario, variations of 15% are considered.

It is importantly noted that this sensitivity analysis considers possible variation or modification in the LPG price, the electricity tariff (to the battery scrubber system), and the H_2 price. Error ranges of these values are utilized, as shown in Table 1. When the optimistic and the pessimistic scenarios are considered, these ranges also vary within each scenario. Considering specifically the proposed H_2 scrubber system, the variation in Al source is also considered. This is expressed within the SED range, as also shown in Table 1. The cost of NaOH to elaborate the solution is included in the OpEx.

From Table 2, for all scrubbers examined, it is clarified that the highest costs are those of the OpEx, followed by the SED and DTCs. It is remarkable that the OpEx costs are determined based on the CapEx costs following a parametric cost estimate (or factored method) [52]. Although it is recognized that the OpEx is constituted by fixed and variable costs, an annual percentage based on CapEx values is considered, i.e., 3%, 1% and 0.75%, respectively [53–55]. These percentages are based on previous literature concerning the matter [53–55].

3.3. Carbon Footprints and H_2-Powered In Situ and On-Board Production and Its Perspectives

The global requirements demand sustainable modes to reduce or to eliminate pollutant emissions. Thus, actions to replace vehicles and equipment operating with fossil fuel with

those that do not locally generate CO_2 emissions are required. Certain debates are arising in terms of the carbon footprint. These are leading to more robust data, evidence, analysis and discussions to clarify the "zero-emission" provided by these "alternative sustainable systems" [55,56]. Although sustainable technologies such as battery and hydrogen systems do not directly generate CO_2 at the points of their utilization, or at recharging, or in the production/recycling process, a certain amount of electricity is consumed. Brousek et al. [55] and Joshi et al. [56] have also stated certain discussion detailed mixture among the energetic systems in Central Europe and in India. As also previously reported [23–26], an H_2-powered scrubber involving hybrid sustainable systems has solar/photovoltaic to supply the electricity to promote the electrolysis and/or water splitting. Subsequently the hydrogen is guided (in-taking) to the fuel cell. In certain applications, a battery pack integrated in the system is required, and complementarily, an advanced electronic circuit to control and to modulate the high power is also demanded [23–26]. From this point of view, those aforementioned total costs and the CO_2 emissions should obligatorily be added and integrated. This is used to equalize or to balance the utilization time of each sub-system integrating the main hybrid system. This becomes a very expensive system, which financially seems to be a reason for its rejection in future planning. Although three distinct hybrid systems are further discussed, and these are not intrinsic results from this investigation, they are rewritten or designed linearly to facilitate their comprehension and functioning mechanism. Although it is recognized that there are compressed H_2 fuel cell scrubbers [17,23,24], in this present investigation, an "in situ" and "on-board" hydrogen fuel cell scrubber system is intended and proposed.

Figure 2a–c depict the typical schematic representations of three distinct hybrid systems. Figure 2a shows a battery pack supplying energy to the PEMFC. In this system, H_2 is produced and, after energy is converted, the electric power is guided to the AC electric motor system. Li et al. [11] have proposed a hybrid system constituted by two subsystems representing a hydrogen-to-electric energy conversion. A PEMFC is the main energy supplier. Due to the high load varying continuously and power being demanded, a dynamic energy transfer is required. This is not fully provided by the PEMFC, since it has a slow dynamic response to load fluctuations. Thus, a battery-pack type lithium-ion state of charge (SOC) is utilized. In addition, the complete circuit includes buses (DC/DC) interfacing to the fuel cell. Thus, management and integration with other components to maintain the bus voltage stability is provided. With this, the load distribution is facilitated [11], as simplified and shown in Figure 2a. Li et al. [11] have simulated and modeled three different operational scenarios and the modeling is optimized [11].

Figure 2b shows another hybrid system constituted by three subsystems, i.e., the first (1) is the motor system, (2) is the PEMFC subsystem and finally, the third (3) is that of containing a metal hydride (MH) system. Simplifying the explanation, a battery pack interfacing to the PEMFC and the motor with adequate converter and inverter devices is used.

The MH subsystem is a H_2 refueling subsystem constituted by a MH compressor (>350 bar) where the hydrolysis of sodium borohydride ($NaBH_4$ as metal hydride) occurs and H_2 is "stored/pressured" under low-pressure hydrogen (<50 bar). Sequentially, when demanded, a certain portion of H_2 is "equalized" by using a buffer and it is managed in an adequate volume ratio throughout to the dispenser to the PEMFC. The cycle is finalized when H_2 is converted to energy and the DC/AC conversion feeds the AC motor subsystem, as shown in Figure 2b.

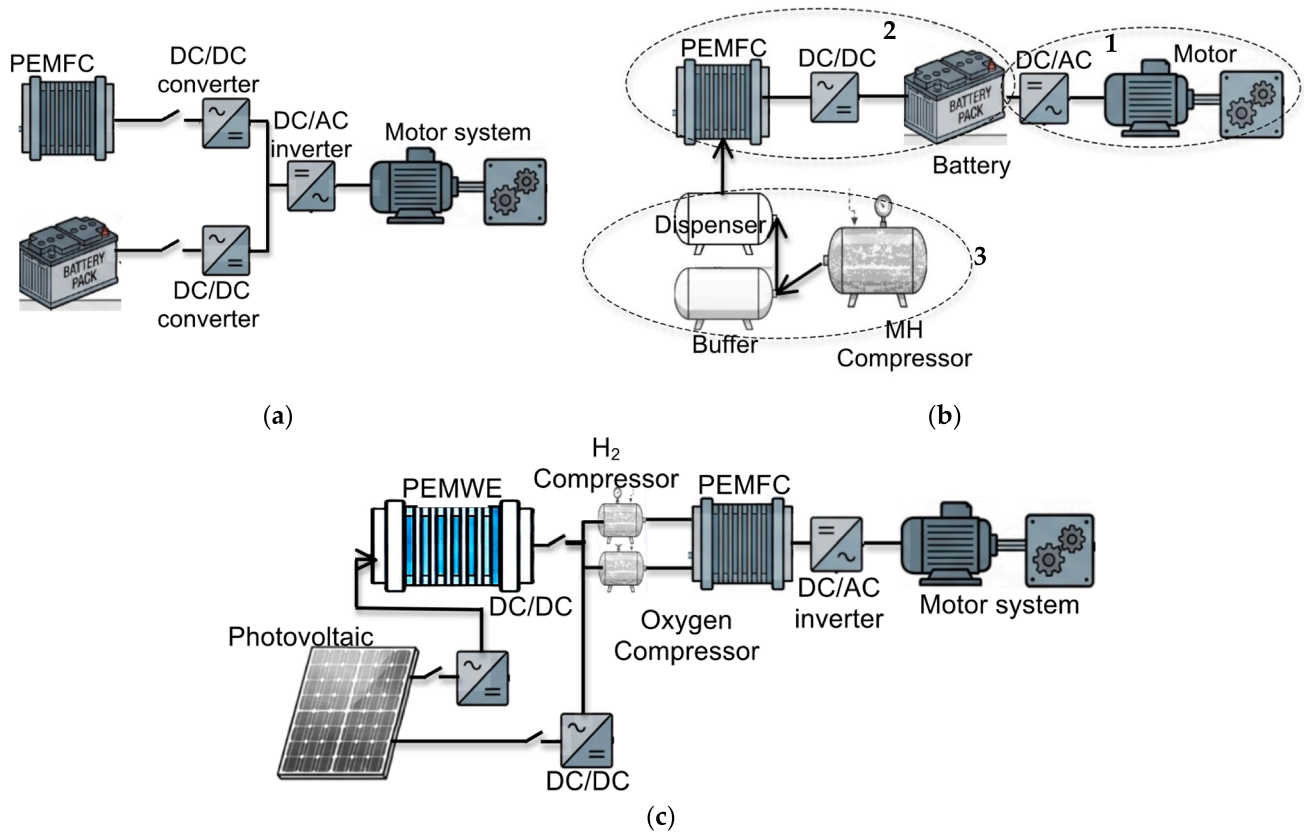

Figure 2. Schematic representations of the hybrid energy sourcing systems: (**a**) a battery pack (type lithium-ion state of charge) integrated with PEMFC and motor; (**b**) a metal hydride (MH) subsystem (3) to produce H_2 into PEMFC integrated to a battery stack (subsystem 2), and the motor (subsystem 1), and (**c**) constituted by the motor subsystem integrated to the PEMFC + PEMWE (proton exchange membrane electrolyzer) with storage tanks (O_2 and H_2); and the photovoltaic arrangement. All systems work using DC/DC converters and DC/AC inverters.

Yartys et al. [17,23,24] have utilized a similar system. This system is applied in a forklift machine [17]. Evidently, other additional technical details are required. For instance, an advanced electronic control unit (ECU) with PWM (pulse width modulation) and microcontrollers and supercapacitors are obligatorily required. With this, the electric load is managed or modulated to AC or DC motor setting the electric pulses instead of severe fluctuations in voltage. This provokes certain damage to the battery and the PEMFC. A typical schematic representation of another type of hybrid system is depicted in Figure 2c. This can be simply interpreted or visualized as four different subsystems, i.e., the motor + inverter; the PEMFC; the PEMWE (proton exchange membrane electrolyzer) with the storage tanks (O_2 and H_2); and the photovoltaic array. Zhang et al. [15] have modeled a similar system designated as a photovoltaic–electrolyzer–fuel cell system. Different from that shown in Figure 2a,b, this depicts a hydrogen production system utilizing a water electrolysis device.

In the PEMWE, water is fed to the anode and decomposes into oxygen gas, protons and electrons driven by required electricity [15]. An external voltage is required, which is supplied by the solar photovoltaic subsystem (~28 m^2). The O_2 is generated on the anode and H_2 on the cathode of the PEMWE due to the protons combination with electrons. H_2 production rate is in accordance with the system demand. Zhang et al. [15] have reported that the mentioned system produces a hydrogen rate of about 65 $g_{(H2)}$/h, producing close to 1.6 kWh. The authors have simulated/modeled and validated all the subsystems, evidencing their feasibility for a hybrid system. The system efficiency fluctuates due to the

solar radiation oscillations and shows a reasonable monotonic decreasing trend with the increase in the environmental temperature.

In a general way, it is recognized that all hybrid systems to generate alternative and renewable energy undergo fluctuations depending on their subsystems. This can also be verified in those fossil fuel-powered systems. In this direction, an integrated hybrid system is proposed, constituted by an H_2 generator subsystem modulating H_2 quantities to the PEMFC and modulating the energy to the electric motor system, as schematically shown in Figure 3a,b.

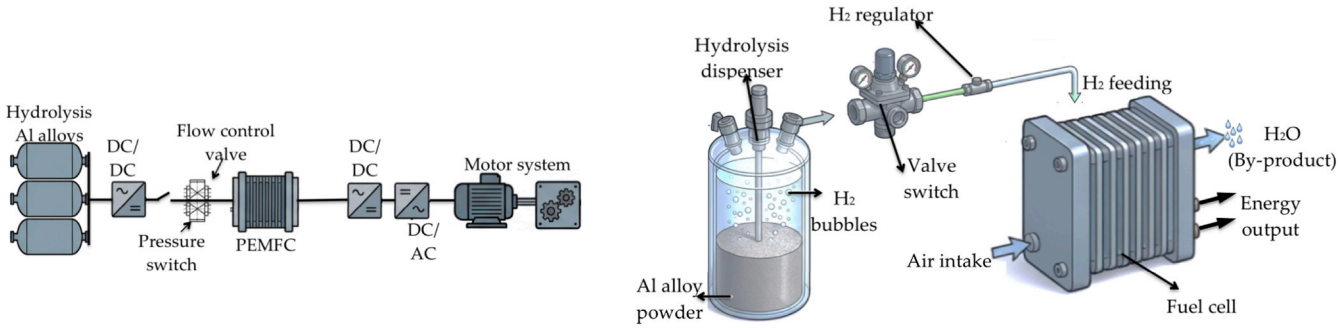

(**a**) (**b**)

Figure 3. (**a**) Schematic representation of the proposed hybrid in situ H_2 generator by using the hydrolysis concept, modulating H_2 quantities to the PEMFC, and (**b**) detailing hydrolysis dispense supplying "on-demand" H_2 by using a pressure switch and flow control valves.

The concept of aluminum-based alloy hydrolysis is adopted to produce "in situ" a certain volume of hydrogen. A flow control valve modulates this, and a pressure switch "feeds" the H_2 adequately to a PEMFC system. Evidently an ECU associated with PWM circuits can also be adopted. This contributes to finer modulation, and possible load demand fluctuations are more adequately controlled. It is recognized that Al hydrolysis reasonably supplies certain hydrogen volume during short-to-longer periods. This is intimately associated with the various operational parameters and characteristics of the hydrolysis system. It can be mentioned that the nature and concentration (molarity) of the electrolyte, temperature of the electrolyte, the type and nature of the selected Al-based alloy, Al weight-to-water/solution ratio, etc. [57–65].

Costa et al. [57] have reported a gamma of articles demonstrating the mechanism to activate Al in water and/or solution. During the last 20 years, binary, ternary and multi-element alloys with portions of solute materials with low melting points are focused in the majority of studies [58–63]. Galvanic couple preconizes Al and its alloys activation in water or alkaline solution (NaOH), which corroborates with the oxide layer dissolution, and the hydrolysis is more efficiently provided [58,59,63–65]. From the metallurgical point of view, Costa et al. [57] have recently contributed to the understanding of the resulting microstructural arrays on the H_2 yield production [57]. Al-Sn and Al-Bi alloys in distinctive chemical compositions and different microstructural morphologies (i.e., cellular and dendritic arrays) are examined. Considering a stagnant and naturally aerated 0.5 M NaOH solution, it is found that the Al-Sn and Al-Bi alloys have opposite H_2 yield productions. The Al-Bi alloys have better H_2 generation results associated with coarser Bi droplets. On the other hand, the Al-Sn alloy samples characterize finer dendritic microstructures. This dendritic microstructure is predominantly characterized by fiber- or plate-like Sn-rich phases. Finer Bi droplets characterize the resulting morphologies of the Al-Bi alloys. These provide cathode-to-anode area ratios (Ac/Aa) with higher anode area. This facilitates the

"corrosion", inducing a better hydrolysis process. It is important to note the role of the selected aluminum-based alloy in the hydrogen yields. It should also be considered that high or low cooling rates substantially affect the H_2 yield results. This suggests that the operational casting parameters can be used to "control" the hydrogen production. It is also suggested that the portion of the H_2 volume can be modulated according to the load and absorb fluctuations occurring in an AC or DC motor. Using supervisory devices and microcontrollers, the modulation or regulation can be stipulated, as schematically shown in Figure 3b.

3.4. Proposed In Situ H_2 Production: Effects of NaOH Ratio vs. Al Powder Mixtures

It is unquestionable that a great number of parameters affect the H_2 yields, and the volume produced can be modulated. In the case of the scrubbers, no high loads or great fluctuations occur or are demanded. When occurring, these are very different, as verified in off-road vehicles or ships, as previously reported [4,11]. These parameters can be intrinsically associated with adopted or selected Al-based alloys or endogenic to the electrolyte utilized, e.g., N_2SO_4, KOH or NaOH [66–68]. The concentration can range between 0.5 M and 5 M. Costa et al. [57] have used a dilute NaOH solution, while Yoo et al. [59] have used a 2 M NaOH solution at different temperatures. Additionally, the Al powder weight-to-volume ratio of the alkaline solution also is other important parameter affecting the hydrogen rate. Figure 4a shows the experimental results using two distinct NaOH molarity (concentration) solutions, i.e., 0.25 M and 0.5 M. Two mixtures between Al + Sn powders are used. Considering 3% and 10% (wt.%) at environmental temperature (~24 °C) and stagnant solution.

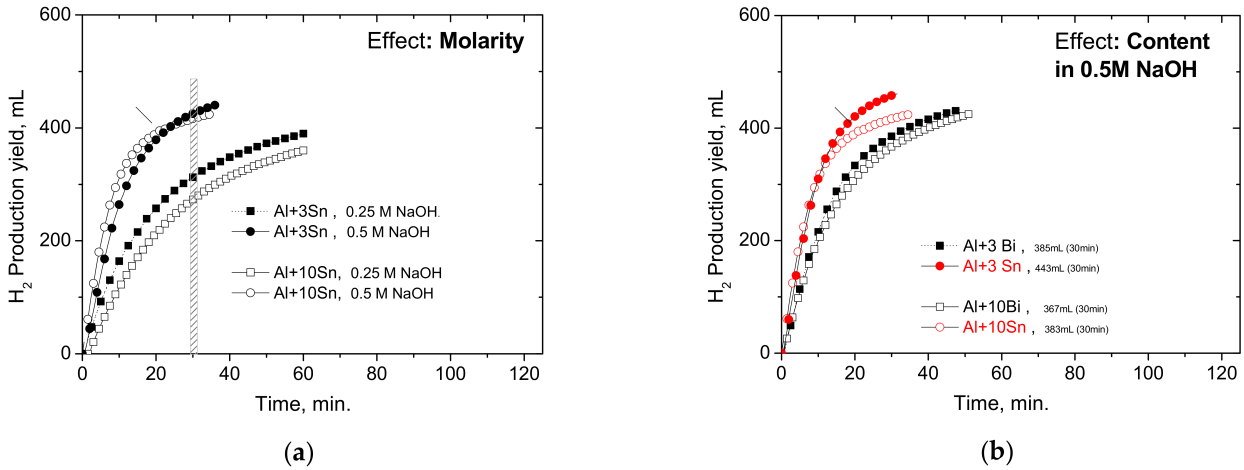

Figure 4. The experimental results of H_2 production yields of two mixtures between Al+Sn powders (3% and 10% wt.% Sn) evidencing the effect of: (**a**) two distinct NaOH molarities (concentrations), i.e., 0.25 M and 0.5 M; and (**b**) distinct mixtures between Al + Sn and between Al + Bi powders.

The effects of the solute contents (3 and 10 wt.%) are also seen in Figure 4a. It is clearly observed that the diluted (0.25 M) NaOH solution promotes lower H_2 production than the 0.5 M solution. For instance, at 30 min of the reaction, the dilute solution promotes about 26% lower H_2 volume than in a 0.5 M NaOH solution. This result is stoichiometrically expected. In a simplified explanation, it has lower reagent contents than the 0.5 M solution. From the chemical point of view, the reaction kinetics also increased when a 0.5 M solution was used. Hiraki et al. [66] and Jung et al. [67] have also reported that the H_2 production increases with the increase in the solution molarity. Remembering that these chemical parameters can also be used to modulate the hydrogen rate.

Figure 4b depicts the experimental results of the four distinctive mixtures between Al + Sn and Al + Bi powders. It is worth noting that the distribution sizes of these utilized metal powders are in the same order of magnitude (between 140 and 250 μm), as also verified in a previous study [57]. In this previous study, the as-cast Al-Sn and Al-Bi alloy powders are utilized. It is clarified that the highest H_2 yields are those of the mixture of the Al+Sn powders. The lowest results correspond with the Al + Bi powders mixture. Also, it is verified that lower concentrations of both the Al+Sn and the Al + Bi mixtures are those corresponding with 3 wt.%. This result is also expected based on the fact that more Al wt.% is correlated with these mixtures. Additionally, from the chemical point of view, Sn has an amphoteric behavior, which also contributes to a slight H_2 production [64,65,69]. Although this contribution is minor to the total produced, this behavior is not verified with Bi additions, which have an inert behavior in NaOH solution at environmental temperature. Although no chemical detail is focused on this discussion, this reasonably provides the understanding of those attained results. In addition, it provides certain guidelines for planning the hydrogen evolution according to the electric demand in a hybrid "in situ" and "on-board" H_2 system.

Figure 5a,b show the experimental results of the hydrogen generation of the Al + 3Bi powders with the reaction time and with the quantity (volume) of 0.5 M NaOH, respectively. It is found that the Al powder–to–NaOH volume ratio substantially affects the H_2 yields attained.

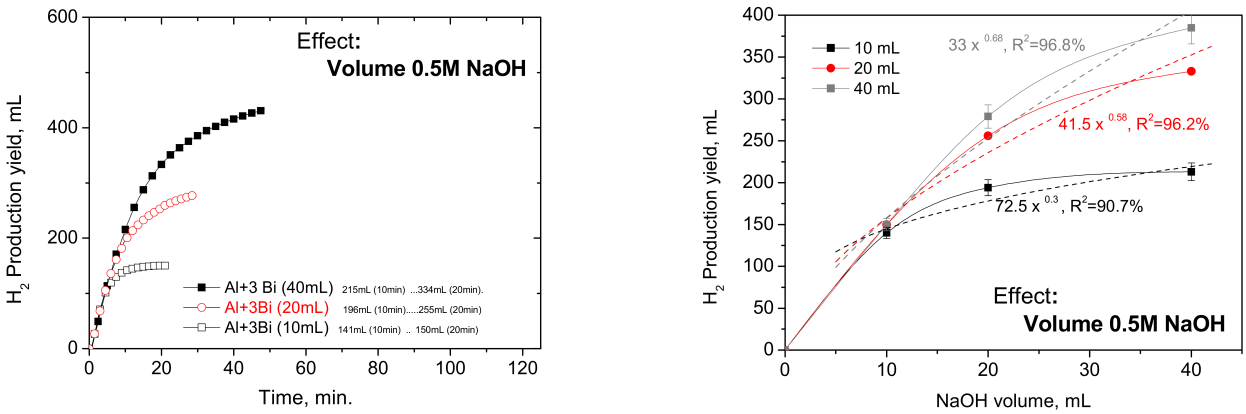

(**a**) (**b**)

Figure 5. The experimental results of the hydrogen production of the Al + 3Bi powders with: (**a**) reaction time in a stagnant 0.5 M NaOH solution at environmental temperature, and (**b**) with different volumes of 0.5 M NaOH defining distinct Al powder–to–NaOH volume ratios.

For instance, when a ratio of 0.4 g Al powder (solid) is used with 40 mL NaOH (liquid) (1:100), the highest H_2 yield is achieved. The worst result is that of the powder-to-solution ratio of 1:25 (i.e., using 10 mL NaOH and 0.4 g powder), as shown in Figure 5b. This is also another important parameter to plan the modulation of the H_2 feasible for the PEMFC system. Additionally, this also contributes to the distribution and the physical arrangement of the components in the frame and constructional structure of the proposed ride-on industrial floor scrubber. For instance, although a 1:100 ratio (i.e., 0.4 g powder–to–40 mL NaOH) reveals the rapid kinetic reaction providing a higher H_2 rate, a higher volume of the NaOH (~100 L) is demanded. Since in situ H_2 and pressureless hydrogen are intended, the planning of the hydrogen rate is essential to the success of the proposed industrial scrubber system. Based on the assessments previously commented on, it seems that the Al-based alloy selection and volume and concentration of the NaOH are essential keys.

Table 3 shows distinct studies utilizing Al hydrolysis and comparing with the hybrid systems. Also, the effects of the concentration and nature of alkali solution (NaOH or KOH), temperature and solid-to-liquid ratio (i.e., Al quantity per volume of alkali solution) are demonstrated. From each study, data on the H_2 production (in mass or volume per period) are provided. Additionally, the results of the energy (in kW) or its corresponding consumption (in kWh) are commented.

Table 3. Comparison among distinct studies involving Al hydrolysis hydrogen production levels and corresponding energy generated, and comparison with other hybrid energy systems and their energy produced.

Study	System/Quantity	Solution	S/L Ratio	H_2 Production	H_2 (Volume/ Period)	Energy
Hurtubise et al. [20]	Al (1); 22.7 kg	3.5 M NaOH	n/a	2.5 kg	~28,000 (2)	16 kWh 20 kWh
Huang et al. [68]	Al slurry (1); n/a	5 M NaOH	n/a	~3.12 kg (2)	20 L/60 min (200 L -> 15 kwh)	1.5 kW
Srivastava and Meshram [70]	Al dross (1); 3.125 g	1 M NaOH (70 °C)	1:320 (3.125 g/1000 mL)	--	18 mL/min	n/a
		1 M KOH (70 °C)		--	18 mL/min	n/a
		0.5 M NaOH (40 °C)		--	~9 mL/min	n/a
		0.5 M KOH (40 °C)		--	~5 mL/min	n/a
Zhang et al. [15]	Photovoltaic + Electrolyzer + PEM	--	--	65 g/h (~1 g/s)	~12 L/min (2)	1.6 kW
Li et al. [11]	Battery + PEM	--	--	~125 g/min (~2 g/s) (2)	1500 L/min	200 kW
Costa et al. [57]	Al alloys powders (1); 0.4 g	0.25 M NaOH (25 °C)	1:100	--	475 mL/30 min (3) (1190 mL/g)	n/a (983 g(Al)
In this study	Al powders (1); 0.4 g	0.5 M NaOH (25 °C)	1:100	--	385 mL/30 min (4) (963 mL/g)	5~7 W (5) 1000 g Al
		0.5 M NaOH (25 °C)	1:25	--	150 mL/30 min (4) (375 mL/g)	2.3~2.7 W (5)
		0.25 M NaOH (25 °C)	1:100	--	313 mL/30 min (4) (783 mL/g)	4.7~5.5 W (5) 1 kg 2.8 kWh

(1) H_2 produced by using Al electrolysis in alkali solution. (2) Values calculated based on 0.083 g/L, and 0.0899 g/L (at environmental temperature). (3) Values considering the as-cast Al-3 wt.% Bi alloy powders. (4) Values considering the Al powers + 3(wt.%) Bismuth powders. (5) Values determined by using theoretical LHV (lower heating value) and HHV (higher heating value).

Hurtubise et al. [20] have utilized Al hydrolysis in a 3.5 M NaOH solution. It is found that 22.7 kg of Al produced 2.5 kg of H_2. Considering a PEM (50% yield), a range of energy between 16 kWh and 20 kWh is achieved. When calculating the theoretical energies provided by this 2.5 kg of H_2, using both LHV (lower heating value) [69] and HHV (higher heating value) [69], are 83 and 98 kWh, respectively. Although it is considered a PEM (50%), the theoretical values are slightly higher than those mentioned in the study [20]. This seems to be correlated with the "effective efficiency" due to possible energy losses into the system. The following examples are mentioned: the lost energy to initiate the electrochemical reaction, the ohmic drop due to the PEM's materials, the partial heat produced, and the losses due to the peripheral devices for the intrinsic conversion of the H_2 production hybrid system. It is recognized that promoting comparisons among the distinctive systems is very complicated. However, in this direction, it is found that a 5 M

NaOH solution induces a volume of 20 L (H_2) in 60 min. This generates about 1.5 kWh, or 200 L to produce 15 kWh. This results in ~3 kg H_2 being obtained under atmospheric pressure. Comparing with the study developed by Hurtubise et al. [20], it seems that the Al slurry promotes a low efficiency.

When Al dross is used, Srivastava and Meshram [70] have shown that NaOH and KOH solutions at 70 °C have similar results. In dilute concentration and at 40 °C, no proportional decreases in the H_2 production yields are observed. However, it substantially decreases by up to 3.6 times. Considering two very distinct hybrid systems, i.e., photovoltaic + PEMWE + PEMFC, and another constituting battery + PEMFC, the H_2 density is 0.0899 g/L. A 12 L/min hydrogen rate produces ~1.6 kWh, as reported by Zhang et al. [15]. Li et al. [11] have reported that 1500 L/min generates about 200 kW. Mathematically, this suggests that the photovoltaic + PEMWE + PEMFC system seems to be slightly more efficient than the battery + PEMFC. This should be converting about 230 kW instead of those 200 kW. Evidently, this is a simplified approximation, and this possible variation is attributed to the PEM efficiency and its flawless operation/performance. As aforementioned, depending on the selection of the adequate Al-based alloy and/or its composites, the hydrogen production can be substantially different. For instance, when the as-cast Al-3 wt.% Bi alloy powder [59] in a NaOH solution at environmental temperature is used, a similar H_2 volume (16 mL/min) is obtained when a 1 M NaOH solution at 70 °C is utilized [69]. The last rows in Table 2 depict the results obtained in this study, utilizing the Al + Bi powder mixture. It is revealed that the NaOH concentration and the S/L ratio affect the H_2 yields significantly; consequently, the generated energy is affected. Supposing a PEM (50% yielding), when adding 5 g NaOH into 250 mL distilled water (~0.5 M) and utilizing 0.4 g Al mixture immersed into 40 mL of the alkali solution, the converted energies using LHV and HHV [70] are about 5 and 7 W, respectively. When 10 mL of NaOH (0.5 M) is used, the energies converted are 2.3 and 2.7 W, respectively. A practical example concerns this, meaning that a small LED bulb is lighted on during 1 min. Interestingly, when the same 5 g NaOH is diluted into 1000 mL (0.25 M) and 40 mL of this solution is used, the energies of 4.7 and 5.5 W are obtained, respectively. Simplifying, this means that two LED bulbs are lighted on or one bulb is lighted on during 2 min.

Considering the proposed in situ ride-on industrial floor scrubber and losses in a PEM system (50%), an energy load of 1.6 kWh is demanded. This implies that the hydrolysis of 1 kg (Al mixture) produces ~2.8 kWh. Considering the PEM efficiency (50%), the energy attained is 1.4 kWh, which is lower than the 1.6 kWh demanded. This suggests that an amount of 3.2 kWh is required to account for the PEM efficiency. Additionally, a 10% variation is also considered as the security variation/coefficient. Thus, a mass of 1493.2 g (Al mixture) is required to produce the H_2 volume necessary to generate the 1.6 kWh required. Since a 100 L NaOH solution is used, this is associated with the plate-fin heat exchanger (air-cooled or water-cooled); the final liquid will attain ~40 and 28 °C, respectively. Evidently, a dispenser to dispose of the aluminate (by-product) is required. The prototype is in the development stage, but due to the industrial design copyrights, the representation is not depicted/divulgated.

When a 0.5 M NaOH solution with the same volume (40 mL) and 0.4 g Al mixture is used, a mass of about 1000 g (Al mixture powders) is required. This evidences ~1.5× lower material mass, which represents substantial economy in various aspects, e.g., CO_2 emission and manufacturing costs. Similar calculation using the as-cast Al-Bi alloy indicates that only 983 g are required. This clarifies that the adopted Al-based alloys or mixtures have very important roles in feasible H_2 on-demanding condition to the PEM system.

4. Conclusions

In order to propose the H_2-powered industrial ride-on scrubber (IRoS) with in situ and on-board H_2 production, some types of hybrid renewable energy sources are revised and discussed. Conventional liquefied petroleum gas (LPG), an electric battery ($LiFePO_4$), and a hydrogen-powered IRoS are discussed. The energy consumption, the operational costs, the environmental impacts, and the investment paybacks are evaluated. Based on certain assertions, the following conclusions can be drawn:

1. Comparisons among the TCO (Total Cost of Ownership) of the three types of scrubbers (i.e., the LPG, battery and H_2) reveal that the initial purchase of an H_2-powered scrubber is relatively expensive, i.e., about 3× and 1.8× higher than the LPG and battery systems. The highest relative TCO during 10 years is that of the H_2-powered scrubber. A period higher than 8.8 years is demanded to "equalize" costs and gains between the battery- and LPG-powered systems.
2. Considering the static paybacks, in order to replace an LPG machine with the battery-powered one, and the LPG-powered with an H_2-powered scrubber, periods higher than 3 years and 5 years are demanded. When the dynamic paybacks are considered, these periods are higher than 7.4 and 9.4 years, respectively.
3. Other important financial parameters are determined. These involve the SED (specific energetic demand) costs and the downtime for refueling, considering a period of 10 years. The highest SED cost is that of the LPG-powered scrubber, attaining a range between USD 104k and 187k. The corresponding SED values of the battery- and the hydrogen-powered scrubbers are substantially lower (~4% and 7%, respectively) than those of LPG. When the downtime costs (DTC) are evaluated, over 10 years, the LPG-powered machine attains an intermediate value, i.e., between ~USD 350 and 540. The lowest, between ~USD 26 and 128, is that of the H_2-powered scrubber. When the DTC of the battery-powered is considered, the resulting cost can be catastrophic. This is associated with the type and the charging efficiency of the battery packs involved, i.e., the DTC varies between ~USD 0.9k and ~58k.
4. During 10 years, the calculated CO_2 emissions corresponding to the LPG-, battery- and H_2-powered scrubber systems are about 162~194, 10~13 and 5~9 tCO_2, respectively. When the gravimetric energy density (GED) values are estimated, it is found that the LPG-powered system is about two times higher than the battery-powered system, i.e., 1.3 kWh/kg against 0.6 kWh/kg, respectively. Considering the H_2-powered system, this parameter is not favorable (~0.1 kWh/kg). However, when the total weight is taken into account, there exists a similarity to the battery-powered system, i.e., 9.7 Wh/kg against 7.1 Wh/kg, respectively.
5. Considering the CO_2 emissions per gravimetric energy density, the numbers do not favor the LPG-powered system, which produces about 20 kg CO_2 per unit of energy utilized when each kilogram of the machine's structure is also involved. This represents about seven and eight times higher than the other two examined systems.
6. It is concluded that adequate modulation and control of H_2 generated is dependent on Al hydrolysis, which can be helpful to future H_2-powered scrubber planning/designs. For this purpose, three important parameters have essential roles in the successful demanded energy, i.e.:
   - The selection of adequate Al-based alloy or mixture powders;
   - Nature and concentration of alkali solution (molarity);
   - The quantity of solid (Al-based alloy or mixture powders) per volume of alkali solution (liquid), designated as the S/L ratio.

For instance, it is determined that for a demanded energy load of 1.6 kWh, about 1.5 kg of Al mixture powders associated with 100 L of 0.25 M NaOH are demanded. When 0.5 M is used, only 1 kg of mixture is required. This results in about 1.5× lower material mass, associated with a decrease in the manufacturing costs and reduced CO_2 emission. When an as-cast Al-Bi alloy is used, only 0.98 kg is required to produce the same 1.6 kWh.

Author Contributions: Conceptualization, W.R.O., L.H.C. and R.R.S.; methodology, L.H.C. and R.R.S.; software, R.R.S.; validation, W.R.O., L.H.C., R.R.S. and Y.A.M.; formal analysis, W.R.O., L.H.C., R.R.S. and Y.A.M.; investigation, L.H.C. and R.R.S.; resources, L.H.C., R.R.S. and W.R.O.; data curation, W.R.O., L.H.C., R.R.S. and Y.A.M.; writing—original draft preparation, L.H.C. and R.R.S.; writing—review and editing, W.R.O. and Y.A.M.; visualization, W.R.O., L.H.C., R.R.S. and Y.A.M.; supervision, W.R.O.; project administration, W.R.O. and L.H.C.; funding acquisition, W.R.O. All authors have read and agreed to the published version of the manuscript.

Funding: The financial support provided by FAEPEX-UNICAMP (#2252/23), CAPES (Coordination for the Improvement of Higher Education Personnel), Ministry of Education, Brazil, (Grant #1) and CNPq (The Brazilian Research Council) Grants, #407595/2022-8; #313272/2021-2 and 310010/2020-9.

Data Availability Statement: The original contributions presented in this study are included in the article. Further inquiries can be directed to the corresponding author.

Acknowledgments: These are also provided to Luiz A. Garcia (technical department), who has contributed to technical aspects and equipment organization. Also, acknowledgments are directed to Tennant Company (by its Alfa/Tennant company located at Limeira/SP/Brazil) due to its partnership signed. Acknowledgments are also directed to an anonymous colleague, who is a native speaker, who has significantly contributed to English writing revision.

Conflicts of Interest: The authors declare no conflicts of interest.

References

1. Begáni, M.; Javorská, M.; Bednárová, L.; Molokáč, M. Comparative Assessment of Next-Generation Hydrogen Production Technologies: Insights from Hydrogen Expo Hamburg 2025. *Clean Technol.* **2026**, *8*, 82. [CrossRef]
2. Domingues Matinho, V.J.P. Considerations on Renewable and Sustainable Energy in the Context of the Energy Transition: What Is New? *Clean Technol.* **2026**, *8*, 79. [CrossRef]
3. Ahmed Al-Ali, H.; Tokimatsu, K. Environmental Trade-Offs in Water Sourcing for Hydrogen Production: A Comparative LCA of Desalination, Brine Treatment and Freshwater Pathways. *Clean Technol.* **2026**, *8*, 50. [CrossRef]
4. Hwang, J.; Park, K.; Ryu, H.Y.; Park, J.; Yoon, W.; Son, B.; Lee, S.; Kim, H.S. AI-driven hydrogen fuel cell and battery management system for off-road construction heavy equipment. *Int. J. Hydrogen Energy* **2026**, *223*, 154326. [CrossRef]
5. Zuo, J.; Steiner, N.Y.; Li, Z.; Lv, H.; Yang, D.; Hissel, D. Quantifying degradation in hydrogen fuel cells: A holistic approach. *Renew. Energy* **2026**, *263*, 125515. [CrossRef]
6. Wilberforce, T.; Alaswad, A.; Palumbo, A.; Dassisti, M.; Olabi, A.G. Advances in stationary and portable fuel cell applications. *Int. J. Hydrogen Energy* **2016**, *41*, 16509–16522. [CrossRef]
7. Ma, L.; Sui, S.; Zhai, Y. Investigations on high performance proton exchange membrane water electrolyzer. *Int. J. Hydrogen Energy* **2009**, *34*, 678–684. [CrossRef]
8. Zhang, T.; Meng, L.; Chen, C.; Du, L.; Wang, N.; Xing, L.; Tang, C.; Jiang, H.; Ye, S. Similarities and differences between gas diffusion layers used in proton exchange membrane fuel cell and water electrolysis for material and mass transport. *Adv. Sci.* **2024**, *11*, 2309440. [CrossRef] [PubMed]
9. Zhang, C.; Zhang, Y.; Wang, L.; Deng, X.; Liu, Y.; Zhang, J. A health management review of proton exchange membrane fuel cell for electric vehicles: Failure mechanisms, diagnosis techniques and mitigation measures. *Renew. Sustain. Energy Rev.* **2023**, *182*, 113369. [CrossRef]
10. Zhao, J.; Li, X. A review of polymer electrolyte membrane fuel cell durability for vehicular applications: Degradation modes and experimental techniques. *Energy Convers. Manag.* **2019**, *199*, 112022. [CrossRef]
11. Li, M.; Wang, Z.; Li, Y.; Wang, M.; Han, F.; Long, F.; Ji, Y. Hydrogen-electricity-ship-engine-propeller (HESEP) multi-potential field matching and energy efficiency optimization design for hydrogen powered vessels. *Ocean Eng.* **2026**, *352*, 124722. [CrossRef]
12. Keny, J.K.; Breske, S.; Singstock, N.R. Hydrogen-powered vehicles for autonomous ride-hailing fleets. *Int. J. Hydrogen Energy* **2022**, *47*, 9422–9427. [CrossRef]

13. Miao, S.; Ezawa, T.; Sumita, M.; HArano, K.; Imai, A.; Katayama, N.; Dowaki, K. A hydrogen supply system utilizing PEMFC exhaust heat and modular metal hydride tanks of hydrogen-powered bicycles. *Appl. Energy* **2025**, *401*, 126760. [CrossRef]
14. Shusheng, X.; Qiujie, S.; Baosheng, G.; Encong, Z.; Zhankuan, W. Research and development of on-board hydrogen-producing fuel cell vehicles. *Int. J. Hydrogen Energy* **2020**, *45*, 17844–17857. [CrossRef]
15. Zhang, F.; Wang, B.; Gong, Z.; Zhang, X.; Qin, Z.; Jiao, K. Development of photovoltaic-electrolyzer-fuel cell system for hydrogen production and power generation. *Energy* **2023**, *263*, 12556. [CrossRef]
16. Bhutto, J.B.; Kumar, A.; Kamangar, S.; Arabi, A.I.A.; Hakami, H. Design and performance assessment of a green hydrogen and renewable integrated hydrid industrial microgrid with advanced control strategies considering uncertainties of renewable energy. *Sustain. Comput. Inform. Syst.* **2025**, *48*, 101267. [CrossRef]
17. Yartys, V.; Zavaliy, I.; Berezovets, V.; Priskyy, Y.; Manilevich, F.; Kytsya, A.; Verbovytskyy, Y.; Bubov, Y.; Kutsyi, A. Hydrogen generator integrated with fuel cell for portable energy supply. *J. Phys. Energy* **2023**, *5*, 01514. [CrossRef]
18. Guo, J.; Su, Z.; Tian, J.; Deng, J.; Fu, T.; Liu, Y. Enhanced hydrogen generation from Al-water reaction mediated by metal salts. *Int. J. Hydrogen Energy* **2021**, *46*, 3453–3463. [CrossRef]
19. Abdelhamid, H.N. A review on hydrogen generation from the hydrolysis of sodium borohydride. *Int. J. Hydrogen Energy* **2021**, *46*, 726–765. [CrossRef]
20. Hurtubise, D.W.; Klosterman, D.A.; Morgan, A.B. Development and demonstration ofa deployable apparatus for generating hydrogen from the hydrolysis of aluminum via sodium hydroxide. *Int. J. Hydrogen Energy* **2018**, *43*, 6777–6788. [CrossRef]
21. Matera, F.V.; Gatto, I.; Patti, A.; Passalacqua, E. Fuel cell performance assessment for closed-loop renewable energy systems. *J. Energy Chem.* **2016**, *25*, 531–538. [CrossRef]
22. Guizzi, G.L.; Mano, M.; De Falco, M. Hybrid fuel cell-based energy system with metal hydride hydrogen storage for small mobile applications. *Int. J. Hydrogen Energy* **2009**, *34*, 3112–3124. [CrossRef]
23. Yartys, V.A.; Lototskyy, M.V.; Linkov, V.; Pasupathi, S.; Davids, M.W.; Tolj, I.; Radica, G.; Denys, R.V.; Eriksen, J.; Taube, K.; et al. HYDRIDE4MOBILITY: An EU HORIZON 2020 project on hydrogen powered fuel cell utility vehickes using metal hydrides in hydrogen storage and refuelling systems. *Int. J. Hydrogen Energy* **2021**, *46*, 35896–35909. [CrossRef]
24. von Colbe, J.B.; Ares, J.R.; Barale, J.; Baricco, M.; Buckley, C.; Capurso, G.; Gallandat, N.; Grant, D.M.; Guzik, M.N.; Jacob, I.; et al. Application of hydrides in hydrogen storage and compression: Achievements, outlook and perspectives. *Int. J. Hydrogen Energy* **2019**, *44*, 7780–7808. [CrossRef]
25. Metzger, N.; Li, X. Technical and economic analysis of fuel cell for forklift applications. *ACS Omega* **2022**, *7*, 18267–18275. [CrossRef] [PubMed]
26. Shahzad, A.; Jiang, H.J.; Aguey-Zinsou, K.F. Unitized regenerative fuel cells: Fundamental challenges and advancements. *Renew. Sustain. Energy Rev.* **2025**, *215*, 115631. [CrossRef]
27. Wang, S.; Weber, A.Z.; Peng, X. Advances and prospects to achieve high-performing and durable proton-exchange-membrane unitized regenerative fuel cells. *Curr. Opin. Electrochem.* **2023**, *40*, 101340. [CrossRef]
28. GlobalPetrolPrices.com. Liquid Petroleum Gas (LPG) Prices, Retail (Data File). 2026. Available online: https://www.globalpetrolprices.com/lpg_prices/ (accessed on 4 April 2026).
29. Magnino, A.; Marocco, P.; Saarikoski, A.; Ihonen, J.; Rautanen, M.; Gandiglio, M. Total cost of ownership analysis for hydrogen and battery powertrains: A comparative study in Finnish heavy-duty transport. *J. Energy Storage* **2024**, *99*, 113215. [CrossRef]
30. Burnhan, C.; Gohlke, D.; Rush, I.; Stephens, T.; Zhou, Y.; Delucchi, M.A.; Birky, A.; Hunter, C.; Zhenhong, L.; Shiqi, O.; et al. *Comprehensive Total Cost of Ownership Quantification for Vehicles with Different Size Classes and Powertrains*; Report ANL/ESD-21/4; Argonne National Laboratory: Lemont, IL, USA, 2021. [CrossRef]
31. Chen, X.; Pang, Z.; Jiang, S.; Zhang, M.; Feng, J.; Fu, L.; Shen, B. A novel LH_2/GH_2/battery multi-energy vehicle supply station using 100% local wind energy: Technical, economic and environmental perspectives. *Energy* **2023**, *270*, 126871. [CrossRef]
32. Brazilian Association of Eolic Energy (ABEEólica). *Annual Reports 2023*; ABEEólica: São Paulo, Brazil, 2023. Available online: https://abeeolica.org.br/wp-content/uploads/2024/11/424_ABEEOLICA_RELATORIO-ANUAL-2023_DIGITAL_V3.pdf (accessed on 30 June 2026).
33. Chamber of Commercialization of Electric Energy (CCEE). *Sustainability Reports 2024*; CCEE: São Paulo, Brazil, 2024. Available online: https://www.ccee.org.br/relatoriodesustentabilidade/ (accessed on 30 June 2026).
34. Setiyo, M.; Soeparman, S.; Hamidi, N.; Wahyudi, S. Characteristic of LPG compositions in the fuel line during discharging process. *Int. J. Technol.* **2017**, *1*, 112–121. [CrossRef]
35. Li, H.; Jiang, H.D.; Dong, K.Y.; Wei, Y.M.; Liao, H. A comparative analysis of the life cycle environmental emission from wind and coal power: Evidence from China. *J. Clean. Prod.* **2020**, *248*, 119192. [CrossRef]
36. GHG Protocol (Greenhouse Gas Protocol). Calculation Tools and Guidance. Available online: https://ghgprotocol.org (accessed on 4 April 2026).
37. Ou, L.; Cai, H. *Update of Emission Factors of Greenhouse Gases and Criteria Air Pollutants, and Generation Efficiencies of the U.S. Electricity Generation Sector*; ANL-20/41; Argonne National Laboratory: Lemont, IL, USA, 2020. [CrossRef]

38. ONS National Operator of Electrical System, Operador Nacional do Sistema Elétrico. Available online: https://www.ons.org.br (accessed on 19 July 2026).
39. Saevardottir, G.; Magnusson, T.; Kvande, H. Reducing the carbon footprint: Primary production of aluminum and silicon with changing energy systems. *J. Sustain. Metal.* **2021**, *7*, 848–857. [CrossRef]
40. Farjana, S.H.; Huda, N.; Mahmud, M.A.P. Impacts of aluminum production: A cradle to gate investigation using life-cycle assessment. *Scie. Total Environ.* **2019**, *663*, 958–970. [CrossRef] [PubMed]
41. Ahmad, S.; Steen, J.; Zajac, T.; Azadi, M.; Ali, S.H. Carbon emission in metal manufacturing productivity: A global analysis of aluminium smelting. *Energy Res. Soc. Sci.* **2025**, *129*, 104343. [CrossRef]
42. EPRI, Energy Delivery and Customer Solutions. Economic and Environmental Analysis of Fuel Cell Powered Materials Handling Equipment. 2010. 54p. Available online: https://www.epri.com/research/products/1022494 (accessed on 4 April 2026).
43. Agora Industry. Available online: https://www.agora-industry.org/fileadmin/Projekte/2023/2023-24_IND_H2_Insights_BRA/A-IND_322_12-Insights-H2-Brazil_EN_WEB.pdf (accessed on 30 June 2026).
44. Gischler, C.; Eric, D.; Galeano, P.; Ramírez, M.; Gonzalez, J.; Cubillos, F.; Hartmann, N.; Pradelli, V.; Márquez, J.S.; Gutiérrez, J.A.; et al. *Unlocking Green and Just Hydrogen in Latin America and the Caribbean*; Inter-American Development Bank (IDB): Washington, DC, USA, 2023; Volume 1, pp. 1–42. [CrossRef]
45. Gao, C.; Xu, J.; Jia, M.; Sun, Z. Correlation between carbon emissions, fuel consumption of vehicles and speed limit on expressway. *J. Traffic Transp. Eng. (Eng. Edit.)* **2024**, *11*, 631–642. [CrossRef]
46. Tettamanti, T.; Varga, B.; Rottenstreich, O.; Emanuel, D. On the relationship of speed limit and CO_2 emission in urban traffic. *Transp. Res. Interd. Perspect.* **2025**, *32*, 101513. [CrossRef]
47. U.S. Environmental Protection Agency. Available online: https://www.epa.gov (accessed on 19 July 2026).
48. Natural Resources Canada. Learn the Fact: Fel Consumption and CO_2. Available online: https://natural-resources.canada.ca/ (accessed on 19 July 2026).
49. Bielaczyc, P.; Woodburn, J.; Szczotka, A.; Pajdowski, P. The impact of alternative fuels on fuel consumption and exhaust emissions of greenhouse gases from vehicles featuring SI engines. *Energy Proced.* **2015**, *66*, 21–24. [CrossRef]
50. Nilfisk Brasil. Available online: https://www.nilfisk.com.br (accessed on 4 April 2026).
51. Brousek, J.; Petr, T.; Bradec, P. Comparative analysis of CO_2 emissions from conventional internal combustion engine vehicles, battery electric vehicles, and fuel cell electric vehicles in selected Central European countries. *J. Clean. Prod.* **2026**, *544*, 147706. [CrossRef]
52. Towler, G.; Sinnott, R. *Chemical Engineering Design: Principles, Practice and Economics of Plant and Process Design*; Butterworth-Heinemann: Oxford, UK, 2012.
53. Budiyanto, M.A.; Putra, G.L.; Riadi, A.; Febri, G.A.M.; Theotokatos, G. Techno-economic analysis of natural gas distribution using a small-scale liquefied natural gas carrier. *Sci. Rep.* **2023**, *13*, 22900. [CrossRef] [PubMed]
54. Schmidt, O.; Melchior, S.; Hawkes, A.; Staffell, I. Projecting the future levelized cost of electricity storage technologies. *Joule* **2019**, *3*, 81–100. [CrossRef]
55. Vives, A.M.V.; Wang, R.; Roy, S.; Samllbone, A. Techno-econimic analysis of large-scale green hydrogen production and storage. *Appl. Energy* **2023**, *15*, 1211333. [CrossRef]
56. Joshi, A.; Sharma, R.; Baral, B. Comparative life cycle assessment of conventional combustion engine vehicle, battery electric vehicle and fuel cell electric vehicle in Nepal. *J. Clean. Prod.* **2022**, *379*, 134407. [CrossRef]
57. Costa, D.; Bonatti, R.S.; Bortolozo, A.D.; Poloni, E.; Osório, W.R. Hydrogen yields from the hydrolysis of as-cast and filed powders of Al-Bi and Al-Sn alloys. *Int. J. Hydrogen Energy* **2026**, *200*, 152792. [CrossRef]
58. Fan, M.Q.; Xu, F.; Sun, L.X. Hydrogen generation by hydrolysis reaction of ball–milled Al–Bi alloys. *Energy Fuel* **2007**, *21*, 2294–2298. [CrossRef]
59. Yoo, J.H.; Yun, K.S.; Kalubarme, R.S.; Park, C.N.; Park, C.J. Hydrogen Generation Using the Corrosion of Al-Sn and Al-Si Alloys in an Alkaline Solution. *Met. Mater. Int.* **2014**, *20*, 619–627. [CrossRef]
60. Xiao, F.; Guo, Y.; Li, J.; Yang, R. Hydrogen generation from hydrolysis of activated aluminum composites in tap water. *Energy* **2018**, *157*, 608–614. [CrossRef]
61. Huang, L.; Yu, H.; Chen, C.; Zhou, X. Characterized on hydrogen properties and mechanism of Al–Sn–Bi composite poder in salt solutions. *Int. J. Hydrogen Energy* **2024**, *71*, 1070–1080. [CrossRef]
62. Huang, L.; Yu, H.; Chen, C.; Zhou, X. Effect of temperature on hydrogen generation and hydrolysis mechanism of Al–Sn–Bi composite materials. *Int. J. Hydrogen Energy* **2024**, *49*, 422–432. [CrossRef]
63. Dong, Z.; Yao, W.; Niu, F.; Chen, D.; Huang, Y.X. Hydrogen generation dynamics of the reaction between metal aluminum and sodium hydroxide solution under pressurized condition. *Int. J. Hydrogen Energy* **2026**, *198*, 152795. [CrossRef]
64. Zhang, Y.; Su, Z.; You, Z.; Yang, G.; Li, G.; Jiang, T. Sodium stannate preparation from stannic oxide by a novel soda roasting-leaching process. *Hydrometallurgy* **2014**, *146*, 82–88. [CrossRef]

65. Soler, L.; Candela, A.M.; Macanás, J.; Muñoz, M.; Casado, J. Hydrogen generation from water and aluminum promoted by sodium stannate. *Int. J. Hydrogen Energy* **2010**, *35*, 1038–1048. [CrossRef]
66. Hiraki, T.; Yamauchi, S.; Iida, M.; Uesugi, H.; Akiyama, T. Process for recycling waste aluminum with generation of high-pressure hydrogen. *Environ. Sci. Technol.* **2007**, *41*, 4454–4457. [CrossRef] [PubMed]
67. Jung, C.R.; Kundu, A.; Ku, B.; Gil, J.H.; Lee, H.R.; Jang, J.H. Hydrogen from aluminium in a flow reactor for fuel cell applications. *J. Power Sources* **2008**, *175*, 490–494. [CrossRef]
68. Huang, X.; Gao, T.; Pan, X.; Wei, D.; Lv, C.; Qin, L.; Huang, Y. A review: Feasibility of hydrogen generation from the reaction between aluminum and water for fuel cell applications. *J. Power Sources* **2013**, *229*, 133–140. [CrossRef]
69. Lin, H.; Tong, Q.; Zhou, S.; Liao, C. Optimal Investment Strategy for Off-Grid Offshore Wind Hydrogen Production: Hybrid and Standalone PEM Electrolyzer Configuration Comparison. *Clean Technol.* **2026**, *8*, 45. [CrossRef]
70. Srivastava, A.; Meshram, A. Waste-to-hydrogen production: Recycling aluminium dross in alkali solutions. *Next Ener.* **2026**, *10*, 100498. [CrossRef]

Disclaimer/Publisher's Note: The statements, opinions and data contained in all publications are solely those of the individual author(s) and contributor(s) and not of MDPI and/or the editor(s). MDPI and/or the editor(s) disclaim responsibility for any injury to people or property resulting from any ideas, methods, instructions or products referred to in the content.